Geochemical and paleontological characterization of a new K-Pg Boundary locality from the Northern branch of the Neo-Tethys: Mudurnu – Göynük Basin, NW Turkey

Sanem Açıkalın[1]; Johan Vellekoop[2]; Faruk Ocakoğlu[3]; İ. Ömer Yılmaz[4]; Jan Smit[5]; Sevinç Ö. Altıner[4]; Steven Goderis[6,7]; Hubert Vonhof[5]; Robert P. Speijer[8]; Lineke Woelders[8]; Eliana Fornaciari[9]; Henk Brinkhuis[2]

[1] Badley Ashton & Associates Ltd, Winceby House, Winceby, Horncastle, Lincolnshire, UK
[2] Utrecht University, Marine Palynology, Faculty of Geosciences, Utrecht, The Netherlands
[3] Eskisehir Osmangazi University, Department of Geological Engineering, Eskisehir, Turkey
[4] Middle East Technical University, Department of Geological Engineering, Ankara, Turkey
[5] VU University Amsterdam, Faculty of Earth and Life Science, Amsterdam, Netherlands
[6] Vrije University Brussel, Analytical, Environment and Geo-Chemistry, Brussels, Belgium
[7] Ghent Universty, Department of Analytical Chemistry, Ghent, Belgium
[8] KU Leuven University, Devision of Geology, Department of Earth and Environmental Sciences, Leuven, Belgium
[9] Padova University, Department of Geosciences, Padova, Italy

Abstract

A Cretaceous-Paleogene succession is studied in detail in the Mudurnu-Göynük basin in northwestern Turkey. To characterize the K-Pg transition in this basin, two stratigraphic sections were measured and sampled at high resolution: the Okçular and the Göynük North sections. These sections were analysed for siderophile trace elements, including Ir and other platinum group elements (PGE: Ru, Rh, Pd, Ir, Pt), bulk stable carbon isotopes, calcareous nannofossils, planktic foraminifera and organic-walled dinoflagellate cysts (dinocysts). In this basin, the upper Maastrichtian consists of monotonous grey mudstones, mostly intercalated with turbidites and the basal Danian is characterised by grey mudstones, that are overlain by a rhythmic alternation of limetones and mudstones. The K-Pg boundary is marked by a thin, reddish ejecta layer, characterized by an enrichment of PGE and an abrupt negative shift in bulk $\delta^{13}C$. This ejecta layer is followed by 15 – 17 cm of thick darker, clayey mudstone, the so-called boundary clay. The basal Danian is characterized by grey mudstones that are overlain by a rhythmic alternation of limestones and mudstones. The upper Maastrichtian to lower Danian interval displays a succession of biostratigraphic events, such as the globally recognized spike of the dinocyst taxon *Manumiella druggii* in the Maastrichtian, followed by the extinction of Cretaceous planktic foraminifera at the K-Pg boundary, and a subsequent

rapid succession of First Appearance Datums (FADs) of dinocysts, such as *Senoniasphaera inornata*, *Membranilarnacia*? *tenella* and *Damassadinium californicum* and planktic foraminifera, including *Parvularugoglobigerina eugubina* and *Subbotina triloculinoides* in the lower Danian. Overall the sedimentological and paleontological data suggest that the studied sites in the Mudurnu-Göynük basin were deposited under normal marine conditions, likely in an outer neritic to upper bathyal environment. Our geochemical and biostratigraphic characterization of the K-Pg boundary transition in the Mudurnu-Göynük basin provides a new K-Pg boundary record in the Northern branch of the Neo-Tethys and allows a detailed comparison with K-Pg boundary sections worldwide.

1. Introduction

The Cretaceous-Paleogene (K-Pg) boundary, ~66 million years ago, is characterized by one of the largest mass extinction events in the Phanerozoic (Alroy, 2008; Bambach, 2006). This biotic transition has been known for more than a century (e.g. Phillips, 1860; Hancock, 1967) but the causes for the extinctions have been debated over for a long time. The discovery of anomalously high concentrations of iridium (Ir) and other platinum group elements (PGE) at the K-Pg boundary transition provided the first evidence for an extraterrestrial cause (Alvarez et al., 1980; Smit and Hertogen, 1980). Subsequently, a worldwide ejecta layer with Ni-rich spinel bearing microkrystites and shocked quartz was also found at the K-Pg boundary (Smit, 1999) and a large impact structure (Chicxulub) dating from the K-Pg transition was discovered on the Yucatan peninsula in Mexico (Hildebrand et al, 1991). Despite these multiple lines of evidence, alternative hypotheses for the cause of this mass extinction have been proposed over the last decades. Generally, these alternatives focus on the association of the K-Pg boundary either with multiple impacts and/or with large-scale volcanism during the latest Cretaceous; in the form of the Deccan Traps Large Igneous Province (Keller et al. 2012; Chenet et al., 2009).

Nowadays, there is broad consensus that the K-Pg boundary mass extinction event is related to the impact of a large extraterrestrial body at Chicxulub (Schulte et al, 2010). This impact was one of the most devastating events in the history of life, as it resulted in a sequence of regional and global catastrophs, such as earthquakes, tsunami's, a so-called 'fireball ‑ stage' with ensuing global wildfires, ozone layer destruction, severe acid rain and a global impact winter resulting from dust and sulphate aerosols that were ejected into the atmosphere (Kring, 2007; Vellekoop et al., 2014). In addition, water and CO_2 were produced from Chicxulub target lithologies and the projectile, which could have caused greenhouse warming after the dust, aerosols and soot settled (Kring, 2007). The impact has also been suggested to have caused a major perturbation of the global carbon cycle and significant global climate change (Galeotti et al., 2004, Coxall et al., 2006; Vellekoop et al., 2014).

A unique aspect of the K-Pg boundary catastrophe is the timescale at which these events occurred. The K-Pg boundary catastrophe can be regarded as one of the most rapid events in the history of life. Altough numerous studies provide evidence for the K-Pg boundary impact, its consequences for the global carbon cycle are still under debate (e.g. Coxall et al., 2006). Especially the fast, millennial-scale biotic and climatic responses to this rapid event are

poorly understood. Only extensive study of the global sedimentary and fossil record can substantially improve our understanding of important biological and environmental changes across the K-Pg boundary, allowing a better discrimination between impact-induced and other, continuous changes.

In the past decades, a variety of different proxies have been applied in an attempt to further unravel the transient global changes and carbon cycle perturbation across the K-Pg boundary (Brinkhuis et al., 1998; Adatte et al., 2002a; Gardin, 2002; Hollis et al., 2003). Many of these studies were focused on specific regions with abundant sedimentary records of the K-Pg boundary transition. Two of these regions that have been studied intensively are Northern Europe, i.e. the 'Boreal' paleogeographic region (e.g. Denmark, The Netherlands, Poland), characterized by a temperate climate at the time of impact, and the Mediterranean, i.e. the Western Tethys (e.g. Tunisia, Southern Spain, Israel), characterized by a subtropical climate during the K-Pg. Several studies have shown that the K-Pg boundary event resulted in migrations of planktic and benthic biota between these regions, likely signifying strong climatic responses to the bolide impact (Brinkhuis et al., 1998; Galeotti and Coccioni, 2002). The exact extent of these migrations is nevertheless poorly understood because only few records are available from the transitional zone between the 'Boreal' and Western Tethys paleogeographic regions. An example of a region that is within this transitional zone is the northern branch of the Neo-Tethys. Unfortunately, only few localities are available in this region and most of these are characterized by a condensed boundary interval or hiatus (e.g. Adatte et al., 2002b; Gedl, 2004; Egger et al., 2009), inhibiting high-resolution studies. This signifies the need for additional K-Pg boundary records in the northern branch of the Neo-Tethys. Amongst the potential regions for such new high-resolution records is the Mudurnu-Göynük Basin in the Central Sakarya Region, Turkey. Recently, a well-preserved K-Pg boundary transition was discovered in this basin, which is described for the first time in this paper.

The International Commission on Stratigraphy defined the base of the Cenozoic Era, Paleogene System, Paleocene Series and Danian Stage as '*at the reddish layer at the base of the 50 cm thick, dark brown clay in a tributary of the Oued Djerfane, west of El Kef, Tunisia, where it coincides with the iridium anomaly and fallout from a major asteroid impact*' (Molina et al., 2006). This mm-scale reddish layer, i.e. the ejecta layer, is typically characterized by an iridium anomaly, small shocked quartz crystals and microspherules,

defined as microkrysties often containing Ni-rich spinels (Smit, 1999), and a directly overlying negative carbon isotope excursion. In addition, this layer is characterized by a mass-extinction level of planktonic foraminifers and calcareous nannofossil. In the present study, the K-Pg boundary is defined in agreement with this definition.

2. Geological Setting

The study area is located in the Mudurnu–Göynük Basin in the Central Sakarya Region, Turkey (Fig. 1). Since the 1930's this region has attracted a lot of researchers due to its key location in constructing the regional geological history, and the presence of outcrops of both Paleo- and Neo-Tethys and continuous successions from the Jurrasic to the Miocene (e.g. Foley, 1938; Stchepinsky, 1940; Şengör and Yılmaz, 1981; Göncüoğlu et al, 2000; Yılmaz et al, 2010). At the beginning of the Jurassic, rifting started on the Sakarya continent – the continent which was bound by the Intra-Pontid Ocean to the north and the Izmir-Ankara Ocean, i.e. the Northern Branch of the Neo-Tethys, to the south - and continued till the Upper Cretaceous (Şengor and Yılmaz, 1981; Saner, 1980). The area became a fore-arc basin in the Turonian–Santonian due to northward subduction of the northern branch of Neo-Tethys (Saner, 1980).

The sedimentary succession of the basin starts on pre-Jurassic metamorphic basement rocks with Lower Jurassic volcanic andvolcanoclastic deposits (Şengör and Yılmaz, 1981) and continues with mainly shelf and pelagic carbonates with occasional turbidites until the Late Cretaceous (Yilmaz, 2008; Yılmaz et al, 2010, Altiner et al, 1991; Fig. 1). In the Late Cretaceous-Danian most of the basin was characterized by slope and basinal deposits (the Yenipazar and Tarakli Formations; Saner, 1980; Altiner et al, 1991; Yılmaz et al, 2010).

An Albian-Campanian age was assigned to the Yenipazar Formation (Saner, 1980). It comprises mainly pelagic carbonates within the Albian-Santonian interval, but is mostly consist of turbiditic-volcano-turbiditic successions in the Cenomanian-Campanian (Saner, 1980; Altiner et al, 1991; Yılmaz et al, 2010). The Yenipazar Formation gradually passes to the Taraklı Formation, which is dominated by mudstones with occasional turbiditic sandstones and thin limestone/marl beds. Late Campanian, Maastrichtian and Danian times covered by these deposits in the study area. The studied Okçular and Göynük North sections comprise the Yenipazar and Taraklı Formations. Superimposed on the Taraklı Formation is the Selvipınar Formation, which is characterized by shallow marine/reefal limestones and usually interpreted to have a middle Paleocene age (Şeker and Kesgin, 1991; Ocakoglu et al, 2007; Ocakoglu et al, 2009).

Across the Mudurnu-Göynük basin, the Taraklı Formation displays a very typical succession of alternating mudstones and limestone beds, in particular in the basal 20 m of the Danian

succession. This succession comprises the K-Pg boundary transition and can be traced across the entire basin, over more than 150 km. This succession was examined in detail in two stratigraphic sections; the Okçular section (40°23'20.74"N, 30°59'23.04"E), measuring a thickness of 720 cm, and the Göynük North section (40°24'40.84"N, 30°46'42.68"E), measuring a thickness of 400 cm.

3. Material and Methods

For this study, three different sample sets have been used. The Okçular section was initially sampled in 2006 for a basic stratigraphic pilot study with a m-scale resolution on a wider time span and after the K-Pg boundary succession was identified in this section, this interval was subsequently logged and sampled in more detail (mostly in dm-scale) in 2010. To increase the sample resolution at Okçular and identify additional K-Pg boundary sections in the basin, a third field campaign was carried out in 2011, involving high-resolution sampling of the Okçular and Göynük North sections (mm to cm-scale). At both localities the K-Pg boundary interval was sampled at a 1-2 cm resolution to attain a high temporal resolution. At the Okçular section the interval from 100 cm below the K-Pg boundary to 160 cm above the K-Pg boundary was sampled continuously. The samples from both sections were split for micropaleontological, palynological, stable carbon isotope and PGE analyses. For the age control of the Okçular and Göynük North sections different fossil groups were investigated. Low-resolution biostratigraphy using calcareous nannofossil and high-resolution biostratigraphy using planktic foraminifera and organic-walled dinoflagellate cysts (dinocysts) were used to generate a detailed biostratigraphy for both sections. Distribution of samples throughout the studied sections is presented in the Figure 2.

The $\delta^{13}C$ isotopic composition, determined for 411cm of the entire 720cm thick Okçular section was derived from 146 samples with a sample interval ranging between 1mm and 3cm. For the siderophile element determination, 10 samples were collected from the K-Pg boundary-bearing 80 cm of the Okçular section, but the PGE analysis focused on only 6 of these. The isotopic signature of the Göynük North Section is represented by fewer samples than the Okçular section. The 180 cm of the Göynük North section comprises 34 samples (with sample spacing between 2 and 15 cm) for isotopic analysis while 7 samples were collected for siderophile element analysis of the 45 cm thick K-Pg boundary-bearing interval (Figure 2).

Palynology sample preparation

A total of 48 samples from the Göynük North section and 45 samples from the Okcular section were processed following standard palynological processing techniques of the Laboratory of Palaeobotany and Palynology (Houben et al., 2011). Briefly, approximately 10 gram of each sample was crushed, oven dried (60°C), weighted and a known amount (10679,

Standard Deviation 5%) of *Lycopodium clavatum* spores were added. The samples were then treated with 10% HCl to remove carbonate components and 40% HF to dissolve the siliceous components. No heavy liquid separation or oxidation was employed. After each acid leaching step, samples were washed with water and centrifuged or settled for 24h and decanted. The residue was sieved over nylon mesh sieves of 250 μm and 15 μm and agglutinated particles or residue were broken up applying 5 minutes of ultrasound. From the residue of the 15-250 μm fraction, slides were made on well-mixed, representative fractions by mounting one droplet of homogenised residue and adding glycerine jelly. The mixture was homogenised and sealed. All slides are stored in the collection of the Laboratory of Palaeobotany and Palynology, Utrecht University.

For the present study, ~25-30 samples per site were studied for palynology. Palynomorphs were counted up to a minimum of 300 dinocysts. The taxonomy of dinocysts follows t Fensome and Williams (2004), unless stated otherwise. A species list with taxonomic notes can be found in Appendix 1.

Planktic Foraminirefa preparation

The samples of the pilot study on the initial Okçular section were processed at the Middle East Technical University, whilst additional Göynük North and Okçular samples were processed at KU Leuven for foraminiferal studies, following standard micropaleontologic procedures. Rock samples were dried in a stove at 60°C for at least 24 hours. Depending on sample size, 4 to 60 grams of dry rock were soaked in a soda solution (50g/l Na_2SO_4). If necessary, the tenside Rewoquat was used to disintegrate strongly lithified samples. After disintegration, each sample was washed over 2 mm and 63-μm sieves. The dry residues were further sieved into three fractions: 63-125 μm, 125-630 μm and >630 μm. The two smaller fractions were intensively scanned for biostratigraphic marker taxa.

Calcareous nannofossil preparation

For the calcareous nannofossil pilot study on the Okçular section, the samples were processed at the Università degli Studi di Padova, Italy, following standard processing techniques for calcareous nannofossil analysis.

Siderophile element determination

The samples were prepared following the procedures described in Goderis et al. (2013). All samples weighed between approximately 7 and 27 g, although sample masses of around 15 g were preferred to avoid nugget effects. The bulk rock samples were fragmented into smaller pieces, ground to powder with a corundum ball mill and thoroughly homogenized.

The concentrations of Cr, Co, and Ni were determined by ICP-MS, after acid digestion of approximately 100 mg of sample at Ghent University (Goderis et al., 2013). Each solution was measured twice and the mean concentrations are given in Table 1. Accuracy was assessed by analysis of certified reference materials BE-N (basalt; CRPG-CNRS, Nancy, France), PM-S (microgabbro; CRPG-CNRS), DNC-1 (dolerite; United States Geological Survey, USGS), and WPR-1 (peridotite; Canadian Certified Reference Material Project, CCRMP).

The concentrations of the PGE and Au were determined via a nickel-sulfide (NiS) fire assay sample preparation technique combined with ICP-MS, following the procedure described in detail in Goderis et al. (2013). The preferred use of large sample masses and external calibration versus a calibration curve ensures good analytical accuracy and reproducibility, relatively low limits of detection and quantification and simultaneous measurement of all PGE (except Os that volatilizes during the procedure applied). All solutions (of ~10 ml) obtained after NiS fire assay pre-concentration were analyzed twice for their PGE content by ICP-MS on separate measuring days. Next to the reference material TDB-1 (diabase) and WPR-1 (altered peridotite) from the CCRMP (certified and recommended; Govindaraju, 1994; Meisel and Moser, 2004), a spinel-bearing serpentinite UB-N from the Vosges Mountains in France that is distributed by the CRPG-CNRS (Nancy, France) for major and trace element analysis but characterized for PGEs (Meisel and Moser, 2004) and a K-Pg boundary ejecta layer at Stevns Klint (SK10) containing 34.7 ± 1.2 ng/g Ir (1s uncertainty) determined by several international laboratories applying neutron activation analysis (NAA) were used for method validation. Calculated uncertinities and values determined for reference materials can be found in Goderis et al. (2013).

Stable isotope determination

Stable isotope analysis was conducted on bulk carbonate samples. The clean surfaces of rock slabs were drilled with a dentist drill to obtain ~250 µg of powdered sample. Measurements of these samples were performed in the stable isotope laboratory of the department of Earth and

Life Sciences at the VU University Amsterdam. Samples were analysed on a Thermo Finnigan Delta+ mass spectrometer equipped with a GASBENCH II preparation device. Approximately 30 microgram of $CaCO_3$ sample, placed in a He-filled 10 ml exetainer vial was digested in concentrated H_3PO_4 at a temperature of 45 degrees Celsius. Subsequently the CO_2-He gas mixture was transported to the GASBENCH II by use of a He flow through a flushing needle system. In the GASBENCH, water was extracted from the gas, by use of NAFION tubing, and CO_2 was analysed in the mass spectrometer after separation of other gases in a GC column. Isotope values are reported as $\delta^{13}C$ relative to V-PDB. The reproducibility of routinely analysed lab $CaCO_3$ standards is better than 0.1 per mille (1SD).

4. Sedimentology

In the Mudurnu – Göynük Basin, the upper Maastrichtian and lower Danian are represented by two different lithological patterns. The upper Maastrichtian is typically characterized by grayish hemipelagic mudstones/siltstones, which are occasionally intercalated by thin turbiditic sandstone beds in the southeastern part of the basin. The turbiditic sandstones reach the K-Pg boundary, but do not occur in the Danian succession. The lower Danian is characterized by an interval of 30-50 m of rhythmic alternations of fine-grained limestones and limey mudstones throughout the basin. In between these two distinct lithological packages, the K-Pg boundary (confirmed by the palaeontological and geochemical data given below) is marked by a 2-3 mm thick reddish clay layer (ejecta layer here after), which is typically overlain by 15 – 17 cm thick darker, clayey mudstone.

4.1. The Okçular section

The studied Okçular section covers 250 cm below and 470 cm above the reddish layer (Fig. 2A). The 190 cm of upper Maastrichtian of the section is represented by an alternation of turbiditic sandstones with grayish mudstones (Figs. 2A and 3A). The upper 55 cm of the Maastrichtian is devoid of sandy beds (Fig. 3B), although in an identical parallel section 400 m further west, turbidites occur up to 20 cm below the K-Pg boundary. The topmost Maastrichtian muds (up to 1 cm below the ejecta layer) contain well preserved complete aragonitic bivalves and ammonite fragments.

The lowermost Danian (basal 17 cm) is represented by darker clayey mudstone on top of the reddish ejecta layer (Fig. 2A). At 17 cm above the ejecta layer another reddish, iron-rich layer is present (Fig. 3C). This second layer also has a thickness of 2-3 mm, sharp bottom and top

boundaries, but is slightly less continuous than the ejecta layer. The thickness of the dark clay layer in between two layers (17 cm) appears constant for at least 20 m at the outcrop.

The first Danian limey mudstone bed, which is 16 cm thick, appears at 120 cm above the ejecta layer. From this level, the Okçular section continues with rhythmic limestone-mudstone alternations (Fig. 3A).

4.2. The Göynük North Section

The studied Göynük North section covers 125 cm below and 275 cm above the K-Pg Boundary (Fig. 2B). Unlike the Okçular section in the eastern part of the Mudurnu – Göynük Basin, the Göynük North section does not contain distinctive turbiditic sandstone beds in the Maastrichtian. However, Maastrichtian mudstones are occasionally more silty, possibly the more distal equivalents of the turbidites in the Okçular section.

At the Göynük North section the K-Pg boundary is also represented by a laterally continuous 2-3 mm thick reddish ejecta layer (Figs. 3D and 3E). This thin ejecta layer is overlain by 16 – 17 cm of thick darker clay layer which becomes less argillaceous upwards, similar to the Okçular section. On top of the dark boundary clay, a lighter coloured mudstone with high carbonate content is present. This 6-7 cm thick limestone bed is a prominent feature in the field and can be traced throughout the area. This bed is overlain by approximately 1 meter of grey mudstones. Higher up in the section, a rhythmic alternation of limestones and mudstones appears, similar to the Okçular section.

5. Biostratigraphy

The initial biostratigraphic assessment of the longer Okçular section was based on a study using calcareous nannofossils and planktic foraminifera based on a low-resolution sampling (Ocakoglu et al., 2007, 2009; Acikalin 2011). The biostratigraphical framework was later improved through a high-resolution analyses of planktic foraminifera and organic-walled dinoflagellate cysts.

5.1. Calcareous nannofossils

Although only 3 of the samples of the low-resolution set fall with the interval studied herein, this assessment provided the first basic biostratigraphic framework for our age model (Fig. 4,

App. A). The presence of the uppermost Maastrichtian markers *Micula murus* and *Micula prinsii* in samples below the boundary clay of the Okçular section (-270 cm and -80 cm) demonstrates that the basal part of the studied interval comprises the upper part of the *Micula murus* Zone (CC26b, Figure 4A). Above the boundary clay at Okçular occurs a succession of Paleocene assemblages characteristic for Zone NP1, with the basal part of this zone dominated by inferred 'disaster' taxa, such as species of the calcareous dinoflagellate cyst genus *Thoracosphaera*. This bloom is considered characteristic for the lowermost Danian *Biantolithus sparsus* Zone (Perch Nielsen, 1981) and is recognized in the lowest sample above the boundary clay at Okcular, at ~1,38 m above the base of the clay. Above this is a succession of Paleocene taxa, such as *Neobiscutum romeinii* and *Cruciplacolithus primus*. Due to the limited number of samples in this pilot, the lowest occurence of the first true Paleocene nannoplankton species (*Neobiscutum romeinii*) is difficult to assess. In the second sample above the boundary (~4 m above the base of the clay) *N. romeinii* is already present. The FAD of the small form of *Cruciplacolithus primus*, occurs at 630 cm above the base of the boundary clay, delineating the base of the *C. primus* Subzone.

5.2 Planktic foraminifera

Planktic foraminifera from the Okçular and Göynük North sections are common to abundant but not well preserved. In general, foraminifera from the Okçular section show a slightly better preservation than from the Göynük North section. Although in some samples dissolution is likely to have caused planktic foraminifera to be almost absent, in most studied samples biostratigraphic markers could be identified, enabling biostratigraphic analysis (Fig. 4, App. A). The lower Paleocene biozonation scheme is based on Berggren et al. (1995), and the zonation by Caron (1985) is used for the upper Maastrichtian. Encountered marker taxa are shown in Figure 5.

The Okçular Section

Only upper Maastrichtian planktic index foraminifer *R. fructicosa* occurs between -150 cm and the base of the boundary clay. *Plummerita reicheli* (= *P. hantkeninoides*) is not observed in this interval. Although the preservation of planktic foraminifera is generally better at the Okçular site than at the Göynük North site, in general, fewer planktic foraminifera are encountered at Okçular than at Göynük North. This may explain why relatively rare marker species such as *Abathomphalus mayaroensis* are not found at the Okçular site, despite better preservation.

Up to 25 cm above the base of the boundary clay, hardly any planktic foraminifera are present, which may be the result of dissolution. Benthic foraminifera are present but not abundant in this zone and are severely weathered, which supports this assumption. Because no marker species can be recognized, this zone is tentatively assigned to Zone P0 (Fig. 4A). At 25 cm above the base of the boundary clay, very small specimens of *Parvularugoglobigerina eugubina* can be distinguished, marking the base of Zone Pα at this depth. It should be noted however, that Zone Pα may be present further down. *P. eugubina* (incl. *P. longiapertura*) is recognized in all investigated samples up to 100 cm above the base of the boundary clay.

At 150 cm above the boundary neither *P. eugubina* nor *Subbotina triloculinoides* is observed, indicating Zone P1a. The boundary between Zone Pα and Zone P1a is probably situated between 100 and 150 cm above the boundary (Fig. 4A). Attempts to refine this zonal boundary have failed however, as the material investigated in between these two levels was too consolidated to retrieve foraminifera.

Subbotina triloculinoides occurs at 200 cm above the K-Pg boundary, marking the base of Zone P1b. This zone reaches at least up to 470 cm above the boundary. At this depth, *Guembelitria cretacea* is no longer observed, suggesting this level to be situated in the upper part of Zone P1b.

The Göynük North Section

Upper Maastrichtian planktic index foraminifera *Abathomphalus mayaroensis*, *Contusotruncana contusa* and *Racemiguembelina fructicosa* occur sporadically between -100 cm and the base of the boundary clay. Below -100 cm, no typical upper Maastrichtian markers are observed. The uppermost Maastrichtian marker *P. reicheli* is not observed in any of the samples.

The transition across the K-Pg boundary is sharp. There is very little obvious reworking of Cretaceous material into the Paleocene. Common Cretaceous specimens occur at 1 cm above the base of the boundary clay but are very rare at 2 cm and higher above the boundary. Until 20 cm above the base of the boundary clay no *P. eugubina* could be observed, which indicates Zone P0. At 20 cm above the base of the boundary clay the first, strongly weathered *P. eugubina* (incl. *P. longiapertura*) specimens occur, indicating Zone Pα (Berggren et al., 1995).

Neither *S. triloculinoides* nor *P. eugubina* is observed in the interval between ~100 to ~200 cm above the boundary. Therefore, it is assumed that this zone represents Zone P1a (Fig. 4B). It should be noted however that the preservation of this part of the section is very poor, leaving little trace of wall texture or architectural features. Often only partial molds or compressed shells are recognized. It is therefore not possible to assign any biozone with certainty to this part of the section.

5.3 Organic-walled dinoflagellate cysts

The palynological samples from the Mudurnu-Göynük basin yielded an abundance of well-preserved palynomorphs. The assemblages are dominated by dinocysts, with minor contributions of acritarchs, prasinophytes, organic foraminiferal linings and terrestrial palynomorphs (i.e. pollen and spores). Dinocyst ranges are provided in Figure 6 and Appendix A whereas encountered marker taxa and other common taxa are shown in Figure 7.

The Okçular Section

The taxon *Disphaerogena carposphaeropsis*, which has its First Appearance Datum (FAD) at about 1 million years before the boundary (De Gracianski et al., 1998; Williams et al., 2004), is common throughout the studied interval. *Disphaerogena carposphaeropsis* var. *cornuta*, a marker for the uppermost Maastrichtian and Danian (Vellekoop et al.,2014), is present in the upper 80 cm below K-Pg boundary (Fig. 6A). *Manumiella druggii*, which has its FAD ~800 kyr befor the boundary (Williams et al., 2004), is present in the upper 120 cm below the K-Pg boundary, occurring in an acme at ~30 cm below the boundary. The basal Danian is characterized by the Lowest Occurences (LOs) of *Senoniasphaera inornata* and *Cerodinium mediterraneum* at 2.5 cm above the boundary, the LOs of *Membranilarnacia*? *tenella* and *Hafniasphaera septata* at 4.5 cm above the boundary and the subsequent LOs of *Damassadinium cf. californicum*, *Damassadinium californicum* and *Lanternosphaeridium reinhardtii* at 9.5 cm, 12.5 cm and 29.5 cm above the base of the boundary, respectively (Fig. 6A).

The Göynük North Section

At the Göynük North section, *D. carposphaeropsis* is encountered in the upper 100 cm below the K-Pg boundary. *D. carposphaeropsis* var. *cornuta*, has a FAD at 30 below the boundary. The marker species *M. druggii* is present in the upper 70 cm below the boundary, with the

characteristic acme peaking at 40 cm below the boundary (Fig. 6B). The placement of these stratigraphic events suggests that compared to the Okçular section, the uppermost Maastrichtian is slightly more condensed at the Göynük North section, in line with the presence of intercalated turbidites at Okçular.

Similar to the Okçular section, the basal Danian of the Göynük North section is characterized by a succession of FADs of dinocyst marker taxa, with the FADs of *S. inornata* and *Membranilarnacia*? *tenella* at 3 cm above the boundary, the FADs of *D. cf. californicum* and *L. reinhardtii* at 6 cm above the boundary and the subsequent FADs of, *Carpatella cornuta*, *Hafniasphaera septata* and *D. californicum* at 20 cm, 40 cm and 125 cm above the base of the boundary, respectively (Fig. 6B). These last three stratigraphic markers are nevertheless very rare at this section, so the FADs of these taxa are probably not reliable as stratigraphic indicators.

5.4 Biostratigraphic discussion

At both studied sections the Maastrichtian interval is characterized by global biostratigraphic markers for the uppermost Maastrichtian, such as the calcareous nannofossils *M. murus* and *M. prinsii*, the planktic foraminifera taxa *A. mayaroensis*, *C. contusa* and *R. fructicosa* and the dinocyst taxon *Disphaerogena carposphaeropsis*. In addition, at both sites a bloom of the dinocyst marker taxon *Manumiella druggii* was observed. This spike of *Manumiella* is recognized in the uppermost Maastrichtian at Cretaceous-Paleogene sections worldwide (Habib and Saeedi, 2007).

Although the uppermost Maastrichtian planktic foraminiferal marker *P. reicheli*, indicative of latest Maastrichtian Biozone CF1 (Pardo et al., 1996), is not observed in any of the samples, our combined biostratigraphic assessment indicates that at the Okçular and Göynük North sections the uppermost Maastrichtian is stratigraphically complete.

While *P. reicheli* is commonly found in the upper Maastrichtian of the Tethyan realm, for instance in Tunisia (e.g. Speijer and van der Zwaan, 1996; Keller, 2004), Egypt (e.g. Speijer and van der Zwaan, 1996), Spain (Molina et al., 1996) and Israel (e.g. Adatte et al., 2005), its occurrence may be rare and or absent at other sites (e.g. Keller, 2004). *P. reicheli* is for example not found in Kazakhstan (Pardo et al., 1999). The absence of this taxon in the investigated samples may be caused by the rarity of the taxon at this location.

The Danian interval of the Okçular and Göynük North sections displays a succession of regional and global stratigraphic events, such as the FADs of dinocyst marker taxa *Senoniasphaera inornata*, *Membranilarnacia*? *tenella* and *Damassadinium* cf. *californicum* and the FADs of planktic foraminifera taxa such as *P. eugubina* and *S. triloculinoides*, allowing a precise zonation of this interval and confirming the placement of the K-Pg boundary at the reddish layer at the base of the dark clay layer encountered at the Göynük North and Okçular sections (see Fig. 4 and 6).

5.5 Other paleontological findings

The K-Pg boundary succession in the Mudurnu-Göynük basin is characterized by a relative low abundance of macrofossils. Across the K-Pg boundary interval at both sections, the monotonous mudstones occasionally comprise small bivalves and bivalve, gastropod and ammonite fragments. Below the boundary are very rare occurrences of large specimens of the echinoid *Echinocorys edhemi*. In the first meter above the K-Pg boundary, small specimens of the genus *Echinocorys* and other echinoid genera become slightly more abundant. The interval with limestone-mudstone alternations is characterized by the abundant occurrence of larger specimens of *E. edhemi* and at some horizons also by abundant burrows, attributed to a typical *Cruziana* ichnofacies.

6. Geochemistry

6.1. Carbon isotopes

The Cretaceous–Paleogene transition at both sections is characterised by an abrupt negative shift in bulk $\delta^{13}C$ curve just above the ejecta layer (see Fig. 4). At the Okçular section, the bulk carbon istope curve is obtained from 146 samples (App. C). Typically $\delta^{13}C$ values range between -0.93‰ and 0.15‰ at pre-impact sediments and exhibit an abrupt shift from 0.15‰ to -1.6‰ at the ejecta layer. The $\delta^{13}C$ profile of the Okçular section stays in negative values between the ejecta layer and the second reddish layer. At the second reddish layer $\delta^{13}C$ values exhibit a further negative shift to -2.24‰. After the second reddish layer $\delta^{13}C$ values return to pre-impact isotopic values.

The carbon isotope compositions of the selected 34 samples from the Göynük North Section range between 1.20‰ and 1.53‰ in the Cretaceous period, and exhibits an abrupt negative shift at the ejecta layer from 1.23‰ to -0.05‰. The $\delta^{13}C$ values slightly recover to positive values and stay below 1‰ throughout the first 80 cm of the Danian.

6.2. Siderophile element signals

Enrichment of siderophile elements, and more specifically the platinum group elements (PGEs: Ru, Rh, Pd, Os, Ir and Pt; Fig. 4A), in the ejecta layer is one of the common features of most K-Pg Boundary sections sections (e.g., at Caravaca-Spain, Furlo-Italy, and Stevns Klint-Denmark). The siderophile elements are relatively rare in Earth's crust, as these elements partitioned into the core during planetary differentiation. Therefore, enrichment of those elements in roughly meteoritic ratios generally points towards an extraterrestrial source. In this study, the siderophile element contents were determined in respectively 6 and 7 samples across the K-Pg Boundary at the Okçular and Göynük North sections. At both sites studied, all siderophile elements, including Cr, Co, and Ni, show an abrupt increase at the ejecta layer (Fig. 4, App. C).

At the Okçular section, the Ir concentration reaches up to 7.41 ppb in the ejecta layer, compared to ~0.5 ppb below and ~0.8 ppb above this level. This is fully in range of typical K-Pg boundary concentrations reported for other K-Pg sites in the Neo-Tethys region (e.g., Ir_{max} of 16.62 ppb at Caravaca (Spain), 2.33 ppb at Furlo (Italy), or 1.93 ppb at Siliana (Tunusia); Goderis et al., 2013; Fig. 9). In the second reddish layer, the Ir concentration remains stable at background values (0.77 ppb), while Cr, Ni ,Ru, Pt, and Pd exhibit a slight increase (App. C).

Similar to the Okçular section, the Göynük North section is also characterised by an abrupt increase in all siderophile element contents at the ejecta layer, with an elevated Ir content of 7.23 ppb compared to Ir contents of ~0.3 ppb below and ~0.8 ppb above the boundary layer. A second enrichment above the boundary clay was not observed. At both sections, the CI-type carbonaceous chondrite-normalized PGE pattern (Fig. 8) is relatively unfractionated, indicating the presence of a chondritic component, and comparable to the K-Pg boundary patterns observed for most distal sites worldwide (Goderis et al., 2013).

Although the boundary material shows a clear enrichment in siderophile element content of at least a factor 10 compared to the characterized samples directly above this layer at both Okçular and Göynük North, the Turkish pre- and post-impact sediments are considerably elevated compared to average continental crustal values (Ir = 0.02–0.10 ng/g; Goderis et al., 2013 and references therein), but also to background levels above and below the K–Pg interval at, for instance, Caravaca (Ir = 0.057 ng/g, 60 cm below the K–Pg level; Smit and Hertogen, 1980). Where continental crustal average 126-185 ppm for Cr, 24-29 ppm for Co, and 56-105 ppm for Ni (Goderis et al., 2013 and references therein), most Cr and Ni values reported for the Okçular background are above this range ($Cr_{background}$ = 100-212 ppm, $Ni_{background}$ = 77-174 ppm). This is not the case for Göynük ($Cr_{background}$ = 62-140 ppm, $Ni_{background}$ = 56-132 ppm), although the Ni values for the samples directly below the K-Pg boundary are slightly elevated compared to average continental crustal values. On a plot of Cr versus Ir (Fig. 9), projectile-enriched impactites typically follow the mixing lines between Upper Continental Crust (UCC), Continental Crust (CC2) and chondrites (Goderis et al., 2013 and references therein). Samples from the Okçular and Göynük North sections clearly follow these mixing lines as expected, suggesting the addition of ~2 wt% of extraterrestrial material to the boundary clay. All Okçular section samples consistently exhibit high Cr concentrations, following the uppermost mixing trajectory between continental crust and chondrites. Samples from the Göynük section show a wider range in Cr/Ir ratios. Considering that most samples follow the mixing lines, the observed element profiles at the Okçular and Göynük North sections are the result of element mobility during diagenesis, although a mafic-rich provenance area for the Okçular section is can also be suggested based on the Cr contents. Possibly, proximity to a mafic-rich sediment source area to the south (Acikalin, 2011) could have played a role in the observed compositional differences between Okçular and Göynük North.

7. Paleo-environment

The Maastrichtian and Danian deposits of the Mudurnu-Göynük basin mainly consist of fine siliciclastics with relatively high carbonate content. The influx of siliciclastics suggests the presence of landmasses relatively close to the depositional site, likely from an uplifted accretionary prism related to the initiation of continental crust collision further south (Acikalin, 2011).

Our paleontological records can be used to reconstruct the late Cretaceous-early Paleocene depositional environment in the Göynük basin. Dinocysts assemblages can provide valuable information on environmental parameters such as coastal proximity, sea surface temperature and salinity (Sluijs et al., 2005). Overall, the palynological assemblages at Göynük North and Okçular are characterized by a high percentage of marine palynomorphs, generally >90%, indicating that full marine conditions prevailed. The most dominant group of dinocysts is the *Spiniferites-Achomosphaera group*, comprising all species of *Spiniferites* and the morphologically related genus *Achomosphaera*. In general this group makes up 40-50% of the assemblage (Fig. 10). *Spiniferites* and *Achomosphaera* are commonly considered indicative for a typical shelf environment (Sluijs et al., 2005). The low abundances (generally below 20%) of typical coastal taxa such as *Areoligera*, *Glaphyrocysta* and *Hystrichosphaeridium* suggest a relatively offshore, open marine setting. This interpretation is confirmed by the mostly deep shelf benthic foraminifera fauna and the common presence of the bathyal marker *Gavelinella beccariiformis* in the Maastrichtian part of the Göynük North section, suggesting a deposition at an outer neritic to upper bathyal environment, likely at a paleodepth of 200-400 m. This typical deep-water marker is absent in the Okçular section, suggesting that this section was deposited in a slightly shallower setting, as supported by the more common presence of aragonitic bivalves and ammonite fragments in the Okçular section. The relative monotonous sedimentation of mudstones and relative low abundance of macrofossils at both sites is in accordance with the suggested environment. The overall sedimentological and paleontological data demonstrate that the K-Pg boundary sites in the Mudurnu-Göynük basin were characterized by mixed siliciclastic-carbonate sedimentation under normal marine conditions.

8. Discussion

8.1. Cause for the occurrence of a second reddish layer in the Okçular section

The Cretaceous-Paleogene transition in the Okçular section exhibits two reddish layers separated by a 16-17 cm thick dark clay layer. The paleontological and geochemical analyses show that the first reddish layer marks the K-Pg boundary. Although the second reddish layer is absent in the Göynük North section, the lithological change from darker, clay rich mudstone to a less argillaceous lithology around +17 cm is considered as a correlatable surface of the second reddish layer of the Okçular section.

The K-Pg boundary in the Okçular section is marked by an abrupt increase in Ir content to ~7.4 ppb, which is significantly higher compared to local background and average continental crust values. Although Ir content tends to go back to lower values in the levels above the boundary, it does not entirely return to background levels in the samples between ejecta layer and the second reddish layer. In addition, slight enrichment of particular siderophiles element contents (e.g., Ru, Pt, Co) is evident in the second layer (Fig. 4, App. C). Given the concentration differences between the two reddish layers, it is clear that these intervals are not of similar origin. The sharp bottom boundaries of both layers, the continuity of bedding, and the constant grain size in between two layers do not suggest sediment reworking at the Okçular section. These observations exclude the possibility that the second layer reflects a simple repetition of the ejecta layer through faulting and slumping. Rather, geochemical remobilisation and re-precipitation at the sedimentary transition from boundary clay to normal background hemipelagic carbonates appears a more likely cause for the second reddish layer.

8.2. Comparison of the Göynük North and Okçular with other sections

Our sedimentological, geochemical and biostratigraphic characterization of the K-Pg boundary interval in the Mudurnu-Göynük basin demonstrates that the studied sections comprise stratigraphically complete K-Pg boundary transitions. Furthermore, these new records allow a detailed comparison with K-Pg boundary sections worldwide. The sedimentological and paleontological records of the Okçular and Göynük North sections suggest that these sites are deposited in an outer neritic to upper bathyal environment. Therefore, the K-Pg boundary transition in this basin shows most similarities to other outer shelf and bathyal sites in the Tethys ocean, such as El Melah and El Kef in Tunisia or Caravaca and Agost in Spain (Molina et al. 1996; Adatte et al., 2002a, Fig. 11). All these sites

are characterized by monotonous deposition of muds, interrupted by a dark boundary clay with a reddish ejecta layer at the base. Compared to the El Kef section, the Okçular and Göynük North sections appear to be more condensed (Fig. 11), suggesting that these sections might have been deposited in a different environmental setting, possibly more similar to the Caravaca and Agost sections in Spain (Lamolda et al., 2005). Interestingly, at various K-Pg boundary sites deposited in at an outer neritic to upper bathyal environment, such as Caravaca in Spain and Bjala in Bulgaria, the boundary clay is overlain by a prominent limestone bed at the base of planktic foraminifera Zone Pα (Molina et al,. 1996), a feature that is also prominent at the Göynük North section. This limestone bed is often characterized by an acme of *Thoracosphaera* and other calcareous dinoflagellate cysts, related to the initial resumption of carbonate production.

The palynological assemblages of the Okçular and Göynük North sections also have some similarities with those of the K-Pg boundary GSSP at El Kef, Tunisia and other records in the Western Tethys, but have significantly higher abundances of higher-latitude taxa. Dinocyst taxa that are typical for the 'Boreal' paleogeographic region, such as *Palynodinium grallator* (Schiøler and Wilson, 1993), are present throughout the studied interval. Clearly, the dinocyst assemblages of the Mudurnu-Göynük basin represent a transition between the 'Boreal', temperate region and the subtropical region of Western Tethys, comprising components of both assemblages. Hence, the K-Pg boundary sites in the Mudurnu-Goynuk basin comprise an excellent record of the transitional zone between the 'Boreal' and Western Tethys paleogeographic regions. Therefore, the sedimentary records in this basin might provide essential insights in biotic migrations across the K-Pg boundary interval.

9. Conclusion

In this study a Cretaceous-Paleogene transition is studied in two detailed sections (Okçular and Göynük North sections), in the Mudurnu-Göynük Basin, in northwest Turkey. The sections were analysed for bulk stable carbon isotope, siderophile trace elements, calcareous nannofossil, planctic foraminifera and organic-walled dinoflagellate cysts; sedimentological observations were also carried out to characterise the K-Pg boundary. In the study area, the upper Maastrichtian typically comprise of grey mudstones and intercalated turbides, whereas Danian is characterised by grey mudstones and rhythmic alternation of limestones and mudstones. The K-Pg boundry is marked by a thin (2-3mm thick) reddish ejecta layer which is overlain by 15-17cm thick darker mudstone (boundary clay). Enrichment of platinum group

elements and abrupt negative shift of $\delta^{13}C$ geochemically characterise the K-Pg boundary. The ejecta layer in the Okçular section exhibits high Ir concentration (7.41 ppb) and $\delta^{13}C$ values decrease to -1.6‰ from 0.15‰ pre-ejacta values. Similar to the Okçular section, the K-Pg transition in the Göynük North section is also represented by an elevated Ir concentration (7.23 ppb) and a negative $\delta^{13}C$ shift (from 1.23‰ to -0.05‰). In addition to Ir, all other studied siderophile elements a;so show an abrupt increase in the ejecta layer.

The position of the K-Pg boundary is also confirmed by a biostratigraphic assessment. The globally recognised spike of the dinocyst taxon *Manumiella druggii* in the upper Maastrichtian, the extinction of Cretaceous planktic foraminifera at the ejecta layer, and a subsequent rapid succession of First Appearance Datums (FADs) of dinocysts, such as *Senoniasphaera inornata*, *Membranilarnacia*? *tenella* and *Damassadinium californicum* and planktic foraminifera, including *Parvularugoglobigerina eugubina* and *Subbotina triloculinoides* in the lower Danian are some of the biostratographic events which confirm the position of the K-Pg boundary in the Okçular and Göynük North sections.

In the Okçular section a second reddish layer has been note about 17cm above the ejecta layer and it is belived that geochemical remobilasation and re-precipitation at the sedimentary transition from boundary clay to normal background hemipelagic deposition is the main reason of its occurance.

Our sedimantological, geochemical and biostratographic findings suggests that the studies sections typically deposited in an outer neritic and upper bathyal environment and they are stratigpaphically complete. The palynological assemblages clearly indicate that the Okçular and Göynük North sections represent a transition between the Boreal temperate region and the subtropical region of Western Tethys.

10. Acknowledgements

This study is supported by Commision for Scientific Research Projects, Eskisehir Osmangazi University (ESOGU-BAP; Project no: 200715024), The Scientific and Technological Research Council of Turkey (TUBITAK; Project no:104Y153), the Netherlands Organisation for Scientific Research (NWO open competition grant ALWPJ/09047) and the Research Foundation Flanders (FWO grant G.0B85.13 and G009113). S.G.is a postdoctoral fellow of

the Reserach Foundation Flanders (FWO). The authors would like to acknowledge field assistance of Osman Kir, Matthieu Cartigny and Tjerk Veenstra. We would like to thank to two anonymous reviewers and the Editor in Chief, Eduardo Koutsoukos for their constructive comments.

REFERENCES

Açıkalın, S., 2011. Orta Sakarya Bölgesi Kretase – Tersiyer istifinin kaynak bölge ve iklimsel açılardan incelenmesi. PhD Thesis, Eskisehir Osmangazi University, Turkey, 249 p. *(in Turkish)*

Adatte, T., Keller, G., Stinnesbeck, W., 2002a. Late Cretaceous to early Paleocene climate and sea-level fluctuations: the Tunisian record. Palaeogeography, Palaeoclimatology, Palaeoecology 178, 165-196

Adatte, T., Keller, G., Burns, S., Stoykova, K. H., Ivanov, M. I., Vangelov, D., Kramer, U., Stueben, D., 2002b. Paleoenvironment across the Cretaceous-Tertiary transition in eatern Bulgaria. *in* Koeberl, C., MacLeod, K.G. (eds.), Catastrophic Events and Mass Extinctions: Impacts and Beyond: Boulder, Colorado, Geological Society of America Special Paper 356, 231–251.

Adatte, T., Keller, G., Stueben, D., Harting, M., Kramar, U., Stinnesbeck, W., Abramovich, S., Benjamini, C., 2005. Late Maastrichtian and K/T paleoenvironment of the eastern Tethys (Israel): mineralogy, trace element and platinum group elements, biostratigraphy and faunal turnovers. Bulletin Société Géologique de France 176 (1), 35–53.

Alroy, J., 2008. Dynamics of origination and extinction in the marine fossil record. Proceedings of the National Academy of Sciences 105 (Supplement 1), 11536-11542. DOI: 10.1073/pnas.0802597105

Altıner, D., Koçyiğit, A., Farinacci, A., Nicosia, U. ve Conti, M.A., 1991. Jurassic-Lower Cretaceous stratigraphy and paleogeographic evolution of the southern part of north-western Anatolia (Turkey). Geologica Romana, 27, pp 13-80.

Alvarez, L.W., W. Alvarez, F. Asara et al., 1980. An extraterrestrial cause for the Cretaceous-Tertiary extinction. Science 208 (4448), 1095-1108.

Anderson, R. L., 1987. Practical Statistics for Analytical Chemists. Van Nostrand Reinhold, New York.

Arenillas, I., Arz, J.A., Molina, E., 2004. A new high-resolution planktic foraminiferal zonation and subzonation for the lower Danian. *Lethaia* 37, 79-95

Bambach, R, K., 2006. Phanerozoic Biodiversity Mass Extinctions. Annual Review of Earth and Planetary Science 34, 127–155

Berggren, W. A., Kent, D. V., Swisher, C. C., III, Aubry, M.P., 1995. A revised Cenozoic geochronology and chronostratigraphy. Society for Economic Paleontologists and Mineralogists Special Publication 54, 129–212.

Brinkhuis, H., Bujak, J.P., Smit, J., Versteegh, G.J.M., Visscher, H., 1998. Dinoflagellate-based sea surface temperature reconstructions across the Cretaceous-Tertiary boundary. Palaeogeography, Palaeoclimatology, Palaeoecology 141, 67-83.

Brinkhuis, H., Zachariasse, W.J., 1988. Dinoflagellate cysts, sea level changes and planktonic foraminifers across the Cretaceous-Tertiary boundary at E1 Haria, northwest Tunisia. Mar. Micropaleontol., 13: 153-191.

Caron, M., 1985. Cretaceous planktic foraminifera. *In* Bolli, H.M., Saunders, J.B. and Perch-Nielsen, K. (eds), *Plankton Stratigraphy*: Volume 1, Planktic Foraminifera, Calcareous Nannofossils and Calpionellids. Cambridge (Cambridge University Press).

Chenet, A.-L., Courtillot, V., Fluteau, F., Gerard, M., Quidelleur, X., Khadri, S.F.R., Subbarao, K.V., and Thordarson, T., 2009. Determination of rapid Deccan eruptions across the Cretaceous-Tertiary boundary using paleomagnetic secular variation: 2. Constraints from analysis of eight new sections and synthesis for a 3500-m-thick composite section:Journal of Geophysical Research, 114, B06103.

Coxall, H. K., D'Hondt, S., Zachos, J. C., 2006. Pelagic evolution and environmental recovery after the Cretaceous-Paleogene mass extinction. Geology 34, 297-300

De Gracianski, P. C., Hardenbol, J., Jacquin, T., Vail, P. R., 1998, Mesozoic–Cenozoic Sequence Stratigraphy of European Basins: Society of Economic Paleontologists and Mineralogists Special Publication, SEPM, Tulsa, OK, Vol. 60, 786pp

Doerffel K., 1990. Statistik in der Analytischen Chemie. VEB Deutscher Verlag für Grundstoffindustrie GmbH, Leipzig.

Egger, H., Koeberl, C., Wagreich, M., Stradner, H., 2009. The Cretaceous-Paleogene (K/Pg) boundary at Gams, Austria: Nannoplankton stratigraphy and geochemistry of a bathyal northwestern Tethyan setting. Stratigraphy 6 (4), 333-347

Fensome, R. A., Williams, G. L., 2004. The Lentin and Williams Index of Fossil Dinoflagellages 2004 edition. American Association of Stratigraphic Palynologists Foundation Contr. Series.

Foley, E.J., 1938, Göynük civarında yapılan bir istikşaf gezisi. MTA Enstitüsü Raporu, Derleme No: 786, 17 s.

Galeotti, S., Coccioni, R., 2002. Changes in coiling direction of Cibicides pseudoacutus (Nakkady) across the Cretaceous-Tertiary boundary of Tunisia: palaeoecological and biostratigraphic implications. Palaeogeography, Palaeoclimatology, Palaeoecology 178, 197-210

Galeotti, S., Brinkhuis H., Huber. M., 2004. Records of post–Cretaceous-tertiary boundary millennial-scale cooling from the western tethys: A smoking gun for the impact-winter hypothesis?. Geology 32 (6), 529-532.

Gardin, S., 2002. Late Maastrichtian to early Danian calcareous nannofossil at Elles (Northwest Tunisia). A tale of one million years across the K-T boundary. Palaeogeography, Palaeoclimatology, Palaeoecology 178, 211-231

Gedl, P., 2004. Dinoflagellate cyst record of the deep-sea Cretaceous-Tertiary boundary at Uzgrun, Carpathian Mountains, Czech Republic. *in* Beadoin, A. B. and Head, M. J., (eds), The PalynoIogy and Micropalaeontology of Boundaries. Geological Society, London, Special Publications, 230, 257-273.

Goderis, S., Tagle, R., Belza, J., Smit, J., Montanari, A., Vanhaecke, F., Erzinger, J., Claeys, P., 2013. Reevaluation of siderophile element abundances and ratios across the Cretaceous-Paleogene (K-Pg)

boundary: Implications for the nature of the projectile. Geochimicia et Cosmochimica Acta 120, 417-446

Göncüoglu, M. C., Turhan, N., Sentürk, K., Özcan, A., Uysal, S., Yaliniz, M. K., 2000. A Geotraverse Across Northwestern Turkey: Tectonic Units of the Central Sakarya Region and their Tectonic Evolution. Geological Society, London, Special Publications 173, 139-161

Govindaraju K., 1994. Compilation of working values and description for 383 geostandards. Geostandards Newsletter 18, 1–154.

Govindaraju, K., Roelandts, I., 1993. Second report (1993) on the first three GIT-IWG rock reference samples: anorthosite from Greenland, AN-G; Basalte d'Essey-la-Côte, BE-N; Granite de Beauvoir, MA-N. Geostandards Newsletter 17, 227–294.

Habib, D., Saeedi, F., 2007. The Manumiella seelandica global spike: Cooling during regression at the close of the Maastrichtian. Palaeogeography, Palaeoclimatology, Palaeoecology 255, 87-97

Hancock, J.M., 1967. Some cretaceous-tertiary marine faunal changes. Geological Society, London, Special Publications 2 (1), 91-104. DOI: 10.1144/GSL.SP.1967.002.01.10

Hildebrand, A. R., Penfield, G. T., Kring, D. A., Pilkington, M., Camargo Z., A., Jacobsen, S. B., Boynton, W. V., 1991. Chicxulub crater: A possible Cretaceous/Tertiary boundary impact crater on the Yucatán Peninsula, Mexico. Geology 19 (9), 867-871.

Hollis, C. J., Strong, C. P., Rodgers, K. A., Rogers, K. M., 2003. Paleoenvironmental changes across the Cretaceous/Tertiary boundary at Flaxbourne River and Woodside Creek, eastern Marlborough, New Zealand. New Zealand Journal of Geology & Geophysics 46, 177-197.

Houben, A. J. P., Bijl, P. K., Guerstein, G. R., Sluijs, A., Brinkhuis, H., 2001. *Malivnia escutiana*, a new biostratigraphically important Oligocene dinoflagellate cyst from the Southern Ocean. Review of Palaeobotany and Palynology 165, 175-182.

Keller, G., 2004. Low-Diversity, Late Maastrichtian and Early Danian Planktic Foraminiferal Assemblages of the Eastern Tethys. J. Foram. Res., 34(1), 49-73.

Kellerö G,. Adette, T., Bhowmick, P. K., Upadhyay, H., Dave. A., Reddy, A. N., Jaiprakash, B. C., 2012, Nature and timing of extinctions in Cretaceous-Tertiary planktic foraminirefa preserved in Deccan intertappean sediments of the Krishna-Godavari Basin, India, Earth and Plenetary Science Letters 341-344, 211-221.

Kring, D.A., 2007. The chicxulub impact event and its environmental consequences at the Cretaceous–Tertiary boundary. Palaeogeography, Palaeoclimatology, Palaeoecology 255 (1-2), 4-21.

Lamolda, M. A., Melinte, M. C., Kaiho, K., 2005. Nannofloral extinction and survivorship across the K/T boundary at Caravaca, southeastern Spain. Palaeogeography, Palaeoclimatology, Palaeoecology 224, 27-52

Meisel T., Moser J., 2004. Reference materials for geochemical PGE analysis: new analytical data for Ru, Rh, Pd, Os, Ir, Pt and Re by isotope dilution ICP-MS in 11 geological reference materials. Chemical Geology 208, 319–338.

Mohamed, O., Piller, W. E., Egger, H., 2012. The dinocyst record across the Cretaceous/Paleogene boundary of a bathyal mid-latitude Tethyan setting: Gosau Group, Gams Basin, Austria. Cretaceous Research 35, 143-168.

Molina, E., Arenillas, I., Arz, J.A., 1996. The Cretaceous/Tertiary boundary mass extinction in planktic foraminifera at Agost, Spain. Review of Micropaleontology 39, 225-243.

Molina, E., Alegret, L., Arenillas, I., Arz., J., 2006. The Global Boundary Stratotype Section and Point for the base of the Danian Stage (Paleocene, Paleogene," Tertiary", Cenozoic) at El Kef, Tunisia-Original definition and revision. Episodes 29 (4), 263–273.

Ocakoglu, F., Yilmaz, İ. Ö., Demircanö H., Altıner, Ö. S., Hakyemez, A., İslamoğlu, Y., Tekin, U.K., Önoğlu, N., Yıldız, Aç, Uchman, A., Szulc, A., Açıkalın, S., 2007, Orta Sakarya Bölgesi Geç Kretase-Paleojen Çökellerinin Sekans Stratigrafisi, The Scientific and Technological Research Council of Turkey (TUBİTAK, Project no:104Y153), Final Report, 450pp. *(in Turkish)*

Ocakoğlu, F., Yılmaz, İ. Ö., Açıkalın S., 2009, Orta Sakarya Bölgesi, Kretase – Tersiyer istifinin kaynak bölge ve paleoiklimsel açılardan incelenmesi, ESOGÜ – Bilimsel Araştırma Projeleri, 200715024 no'lu proje Final Raporu. *(in Turkish)*

Pardo, A., Ortiz, N., Keller, G., 1996. Latest Maastrichtian foraminiferal turnover and its environmental implications at Agost, Spain. *in* MacLeod, N. and Keller, G. (eds.), Cretaceous/Tertiary boundary mass extinction: biotic and environmental changes, 139–172 (W.W. Norton & Co., New York).

Pardo, A., Adatte, T., Keller, G., Oberhänsli, H. 1999. Paleoenvironmental changes across the Cretaceous–Tertiary boundary at Koshak, Kazakhstan, based on planktic foraminifera and clay mineralogy. Palaeogeography, Palaeoclimatology, Palaeoecology 154, 3, 247–273

Perch-Nielsen, K., 1981. New Maastrichtian and Paleocene calcareous nannofossils from Africa, Denmark, the USA and the Atlantic, and some Paleocene lineages. Eclogae Geologicae Helvetiae 73, 831–863.

Phillips, J., 1860. Life on the Earth: Its Origin and Succession, first ed. Cambridge, United Kingdom.

Saner, S., 1980. Mudurnu-Göynük Havzasının Jura ve Sonrası çökelim nitelikleriyle paleocoğrafya yorumlaması. TJK Bülteni 23(1), 39-52. *(in Turkish)*

Schiøler, P., Wilson, G.J., 1993. Maastrichtian dinoflagellate zonation in the Dan Field, Danish North Sea. Review of Palaeobotany and Palynology 78, 321-351.

Schulte, P., Alegret, L., Arenillas, I., Arz, J.A., Barton, P.J., Brown, P.R., Bralower, T.J., Christeson, G.L., Claeys, P., Cockell, C.S., Collins, G.S., Deutsch, A., Goldin, T.J., Goto, K., Grajales-Nishimura, J.M., Grieve, R.A.F., Gulick, S.P.S., Johnson, K.R., Kiessling, W., Koeberl, C., Kring, D.A., Macleod, K.G., Matsui, T., Melosh, J., Montanari, A., Morgan, J.V., Neal, C.R., Nichols, D.J., Norris, R.D., Pierazo, E., Ravizza, G., Rebolledo-Vieyra, M., Reimond, W.U., Robin, E., Salge, T., Speijer, R.P., Sweet, A.R., Urrutia-Fucugauchi, J., Vajda, V.,

Whalen, M.T., Willumsen, P.S., 2010. The chicxulub asteroid impact and mass extinction at the Cretaceous-Paleogene boundary. Science 327, 1214-1218.

Sluijs, A., Pross, J., Brinkhuis. H., 2005. From greenhouse to icehouse; organic-walled dinoflagellate cysts as paleoenvironmental indicators in the Paleogene. Earth-Science Reviews 68, 281–315.

Smit, J., Hertogen, J., 1980. An extraterrestrial event at the Cretaceous-Tertiary boundary. Nature 285, 198-200

Smit, J., 1999. The Global Stratigraphy of the Cretaceous-Tertiary Boundary Impact Ejecta. Annual Review of Earth and Planetary Science 27, 75–113

Speijer, R. P., Van Der Zwaan, G. J., 1996. Extinction and survivorship of southern Tethyan benthic foraminifera across the Cretaceous/Paleogene boundary. *in* Hart, M. B. (ed) Biotic recovery from mass extinction events, Geological Society, London, Special Publication 102, 343–371.

Stchepinsky, V., 1940. Göynük-Mudurlu-Nallıhan mıntıkası cevher zenginlikleri hakkında rapor. MTA Enstitüsü Raporu,Derleme No: 1058. *(in Turkish)*

Şeker, H. ve Kesgin, Y., 1991. Nallıhan-Mudurnu-Seben-Beypazarı arasında kalan bölgenin jeolojisi ve petrol olanakları. TPAO Arama Grubu Bşk.Rapor No: 2907, 42p. *(in Turkish)*

Şengör, A.M.C. and Yılmaz, Y., 1981, Tethyan evolution of Turkey: A plate tectonic approach. Tectonophysics, 75, 181-241.

Vellekoop, J., Sluijs, A., Smit, J., Schouten, S., Weijers, J.W.H., Sinninghe Damsté, J.S., Brinkhuis, H., 2014. Rapid short-term cooling following the Chicxulub impact at the Cretaceous-Paleogene boundary. Proceedings of the National Academy of Sciences, 111, 21, 7537 – 7541.

Williams, G.L., Brinkhuis, H., Pearce, M.A., Fensome, R.A., Weegink, J.W., 2004, Southern Ocean and global dinoflagellate cyst events compared: index events for the Late Cretaceous– Neogene. *In* Exon, N.F., Kennett, J.P., and Malone, M.J. (Eds.), *Proc. ODP, Sci. Results,* 189, 1–98

Yılmaz, İ. Ö., 2008. Cretaceous pelagic red beds and black shales (Aptian – Santonian), NW Turkey: Global Oceanic Anoxic and Oxic Events. Turkish J. Earth Sci. 17, 263 – 296.

Yılmaz, İ. Ö., Altıner, D., Tekin, U. K., Tüysüz O., Ocakoğlu, F., Açıkalın S., 2010. Cenomanian – Turonian Oceanic Anoxic Event (OAE2) in the Sakarya Zone, Northwestern Turkey: Sedimentological, cyclostratigraphic and geochemical records. Cretaceous Research, 31, 07 – 226.

FIGURES

Figure 1. (A) Palaeogeopgraphy, (B) location (generalised geology simplified from Altıner et al., 1991) and (C) geological map (simplified from Gedik and Aksay, 2002) of the study area.

Figure 2. Lithology and sample positions for calcareous nannoplankton, planktic foraminifera, palynological, bulk carbon isotope and Platinum Group Elemental analyses on the Okçular and Göynük North sections.

Figure 3. The K-Pg boundary is well pronounced in both sections. In the general (A, B) and detail views (C) of the K-Pg boundary in the Okçular section the ejecta layer is distinctive. The lowermost Danian is represented by darker clayey mudstone on top of the reddish ejecta layer in Okçular section, which is overlain by a second reddish layer (C). At the Göynük North section, the ejecta layer is laterally continuous (D). Lowermost Danian dark clay layers are overlain by lighter coloured mudstone with higher carbonate content (E) at the Göynük North section.

Figure 4. Calcareous nannoplankton zonation, planktic foraminiferal zonation, dinocyst events, lithology, Siderophile element (including PGE) concentrations and bulk stable carbon isotopes at the (A) Okçular section and (B) Göynük North sections.

Figure 5. Plate with upper Maastrichtian and lower Paleocene planktic index foraminifera encountered in this study.
1a, b, c: *Parvularugoglobigerina eugubina* (Luterbacher and Premoli Silva) Okçular, 29-30 cm
2a, b, c: *Parvularugoglobigerina longiapertura* (Blow) Okçular, 49-50 cm
3a, b: *Subbotina triloculinoides* (Plummer) Okçular, 300 cm
4: *Guembelitria cretacea* (Cushman) Okçular, 99-100 cm
5a, b, c: *Abathomphalus mayaroensis* (Bolli) Göynük, -100 cm
6a, b, c: *Abathomphalus mayaroensis* (Bolli) Göynük, -50 cm
7a, b, c: *Contusotruncana contusa* (Cushman; emend. El-Naggar) Göynuk, -100 cm
8: *Racemiguembelina fructicosa* (Egger) Okçular, -100 cm

Figure 6. Stratigraphic distribution of selected dinocyst taxa and bioevents in the (A) Okçular section and (B) Göynük North sections. Planktic foraminiferal zones after Berggren et al., (1995) and Pardo et al. (1996); calcareous nannoplankton zones after Perch Nielsen (1981).

Figure 7. Plate with upper Maastrichtian and lower Paleocene dinocyst marker species and common taxa encountered in this study.
1: *Achomosphaera ramulifera* (Deflandre, 1937) Evitt, 1963. Göynük North, 6 cm, slide 1, EF L39-3. Specimen in ventral view.
2: *Damassadinium* cf. *californicum* (Drugg, 1967) Fensome et al., 1993. Okçular, 34-35 cm, slide 1, EF U28-3. Specimen in right lateral view.
3: *Disphaerogena carposphaeropsis* var. *cornuta.* Göynük North, 100 cm, slide 1, EF E34-3. Specimen in dorsal view
4: *Glaphyrocysta perforata* Hultberg and Malmgren, 1985. Göynük North, 100 cm, slide 1, EF Q30-2. Specimen in dorsal view. Note the apical archeopyle and operculum in situ.
5: *Hafniasphaera septata* (Cookson and Eisenack, 1967) Hansen, 1977. Okçular, 250 cm, slide 1, EF K33-1.
6: *Hystrichosphaeridium tubiferum* (Ehrenberg, 1838) Deflandre, 1937. Göynük North, 100 cm, slide 1, EF U20-2. Specimen in ventral view.
7: *Lanternosphaeridium reinhardtii* Moshkovitz and Habib, 1993. Okçular, 49-50 cm, slide 1, EF N36-2. Specimen in right lateral view.

8: *Manumiella druggii* (Stover, 1974) Bujak and Davies, 1983. Göynük North, -40 cm, slide 1, EF R33-2. Specimen in dorsal view.

9: *Membranilarnacia*? *tenella* Morgenroth, 1968. Göynük North, 275 cm, slide 1, EF Q21-4.

10: *Palynodinuim grallator* Gocht, 1970. Okçular, -120 cm, slide 1, EF G34-3. Specimen in ventral view.

11: *Senegalinium bicavatum* Jain and Millepied, 1973. Göynük North, 100 cm, slide 1, EF N20-2. Specimen in ventral view.

12: *Senegalinium laevigatum* (Malloy, 1972) Bujak and Davies, 1983. Göynük North, 80 cm, slide 1, EF O30-2. Specimen in dorsal view.

13: *Senoniasphaera inornata* (Drugg, 1970) Stover and Evitt, 1978. Okçular, 9,5 cm, slide 1, EF L31-4. Specimen in dorsal view.

14: *Spniferites ramosus* (Ehrenberg 1838) Loeblich and Loeblich 1966. Göynük North, 6 cm, slide 1, EF K22-4. Specimen in antapical view.

15: *Trithyrodinium evittii* Drugg, 1967. Okçular, 29-30 cm, slide 1, EF G31-1. Specimen in dorsal view.

Figure 8: CI- normalized logarithmic plot of PGE and Au concentrations across the Okçular and Göynük North K-Pg boundary sections compared to the average composition of the continental crust (Ir, Ru, Pt, Pd from Peucker-Ehrenbrink and Jahn, 2001; Rh and Au from Wedepohl, 1995).CI values from Tagle and Berlin (2008). Elements are plotted in order of decreasing condensation temperatures. Although the boundary clays of both sections clearly show the highest and most chondritic PGE concentrations, all section samples are elevated in PGE compared to the average continental crust, most markedly for Ir

Figure 9: Cr versus Ir concentrations of terrestrial target rocks compared to the composition of the Popigai impact melt rocks, K-Pg boundary clays from Caravaca (Spain), Furlo (Italy), and Siliana (Tunesia), in addition to the characterized K-Pg boundary clays in this study (Goderis et al., 2013 and references therein). The grey field indicats the most likely mixing trajectories between chondritic projectiles and common terrestrial targets. Numbers represent wt.% chondritic material on the mixing lines. The plot os based on Figs. 1 and 2 of Tagle and Hecht (2006). PUM = primitive upper mantle, MORB = mid-ocean ridge basalt, UCC = upper continental crust, CC = continental crust. The Okçular and Göynük North samples clearly follow the mıxıng line, suggesting an impactite origin.

Figure 10: Abundance distribution of the most abundant dinocyst groups of the Göynük North and Okçular sections. The dinocyst group [***Spiniferites + Achomosphaera***] includes all species within the genera *Spiniferites* and *Achomopshaera*. The dinocyst group [***Pterodinium + Impagidinium***] includes all species within the genera *Pterodinium* and *Impagidinium*. The dinocyst group [**Hexa-peridinioids**] includes all peridinioid taxa with an hexagonal archeopyle, except for species of the genera *Andalusiella* and *Palaeocystodinium*. The group [***Hystrichosphaeridium***] includes all species within the genus *Hystrichosphaeridium*. The dinocyst group [**Gv cysts**] includes all taxa with dorsoventrally compressed cysts. The group [**AP cpx**] includes all species of the genera *Andalusiella* and *Palaeocystodinium*. The group [***Manumiella***] includes all species of within the genus *Manumiella*. The group [**Other dinocysts**] includes all taxa that are not included in any of the previous groups.

Figure 11: A biostratigraphic correlation between the new K-Pg boundary sections from the Mudurnu –Göynük basin and several well-known K-Pg boundary sections in the Tethys: the K-Pg boundary stratotype section of El Kef, Tunisia and the Caravaca section, Spain. Zonation scheme and dinocyst FOs from El Kef are based on Brinhuis and Zachariasse, 1988 and Brinkhuis et al. (1998), Zonation scheme and dinocyst FO's of Caravaca are based on Arenillas et al. (2004) and Brinkhuis et al. (1998).

APPENDICES

Appendix A: A supplementary data detailing the abundances of calcareous nannofosils, planktic foraminifera and organic-welled dinoflagellate cycts.

A.1. Calcareous nannofossil data for Okçular Section

A.2. Planktic foraminifera data for the Okçular Section

A.3. Planktic foraminifera data for the Göynük North Section

A.4. Palynology data for the Okçular Section

A.5. Palynology data for the Okçular Section

Appendix B: Systematic palynology - List of encountered dinocyst species and complexes

Appendix C: Supplementary data for the geochemical results

C.1. $\delta^{13}C$ data for Okçular and Göynük North sections

C.2. Concentrations of Cr, Co, Ni, Ir, Ru, Pt, Rh, Pd and Au, for measured samples of the Okçular and Göynük North sections.

Figure1

Click here to download high resolution image

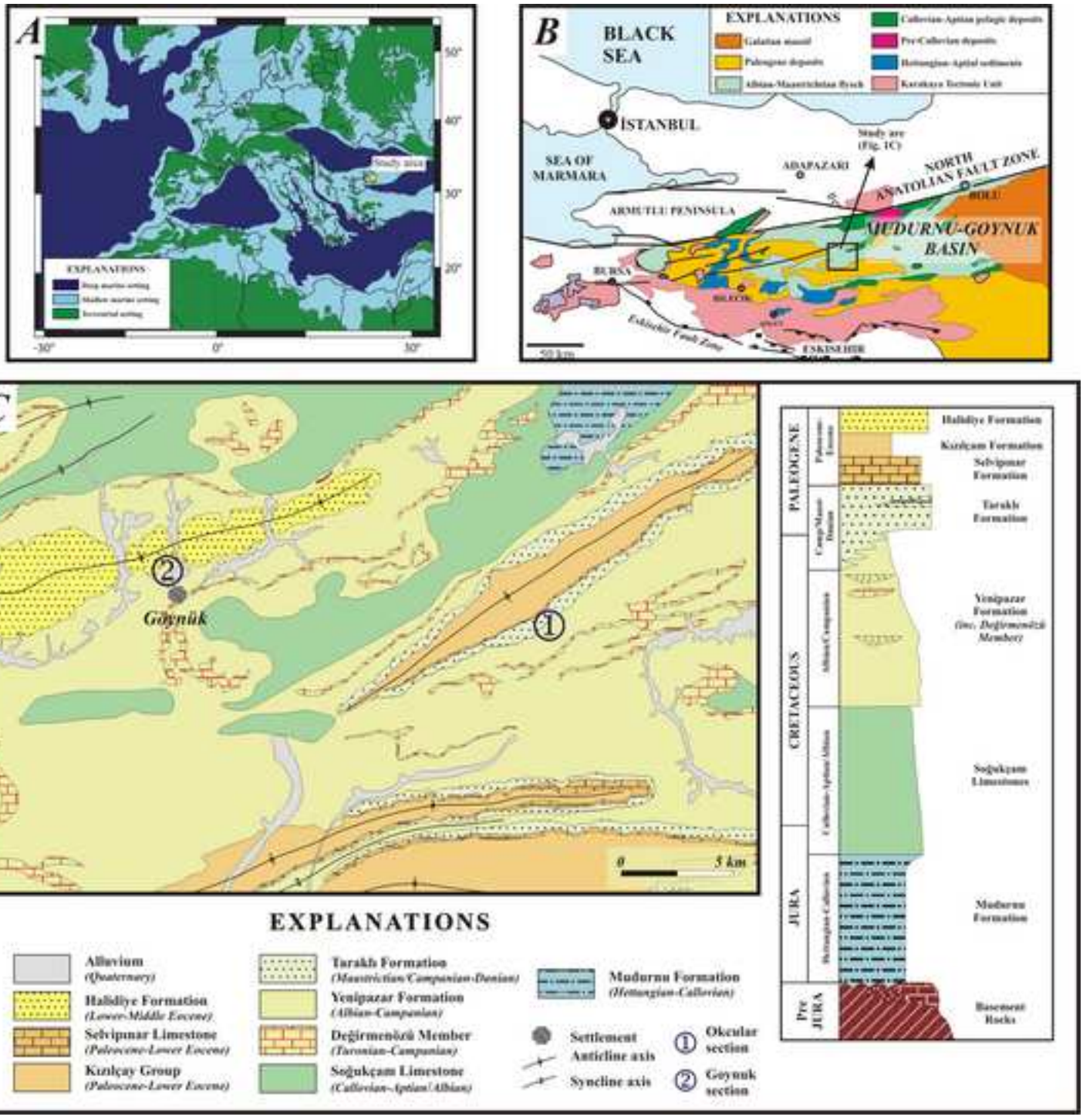

Figure2

Click here to download high resolution image

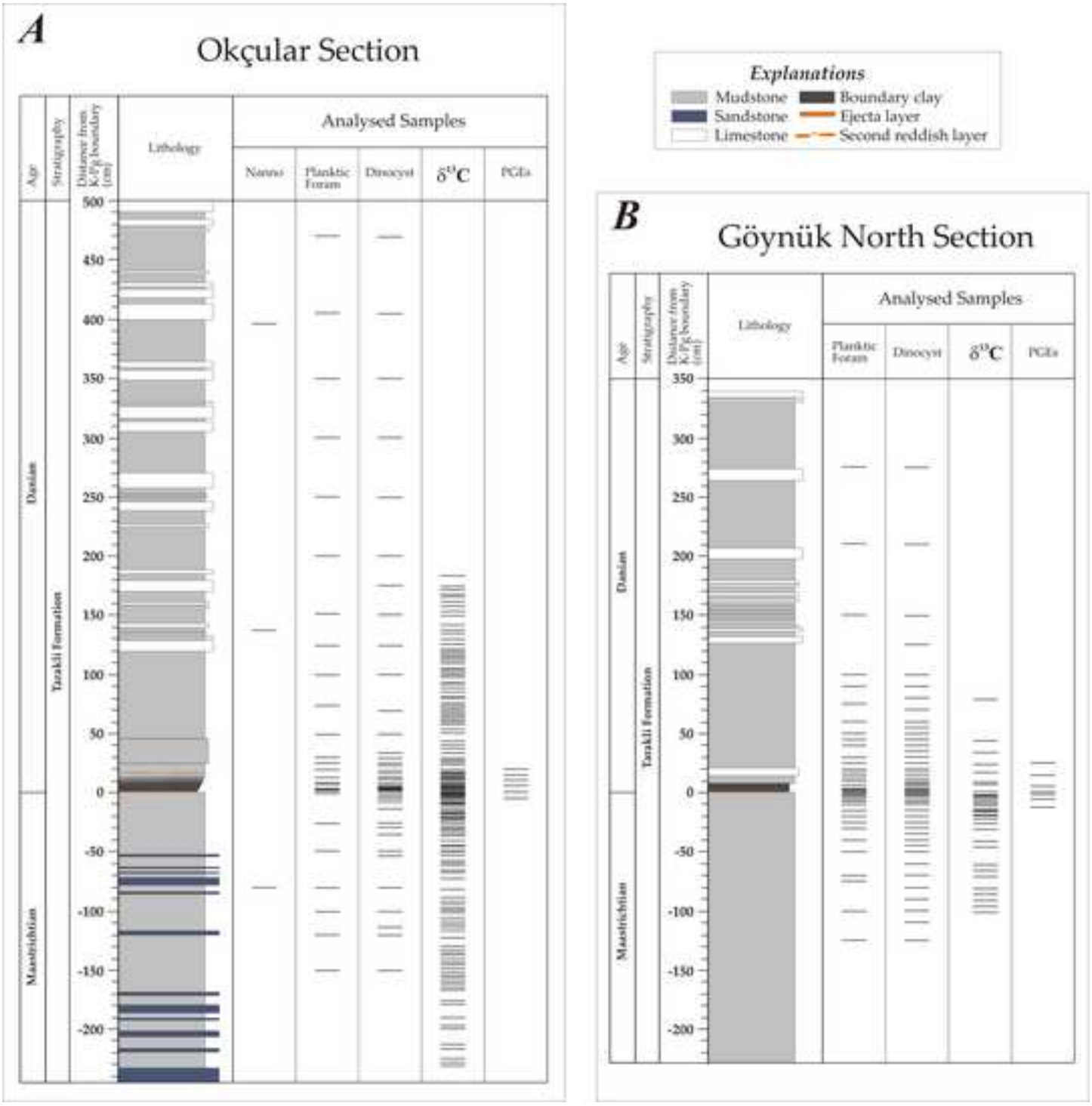

Figure3

Click here to download high resolution image

Figure4

Click here to download high resolution image

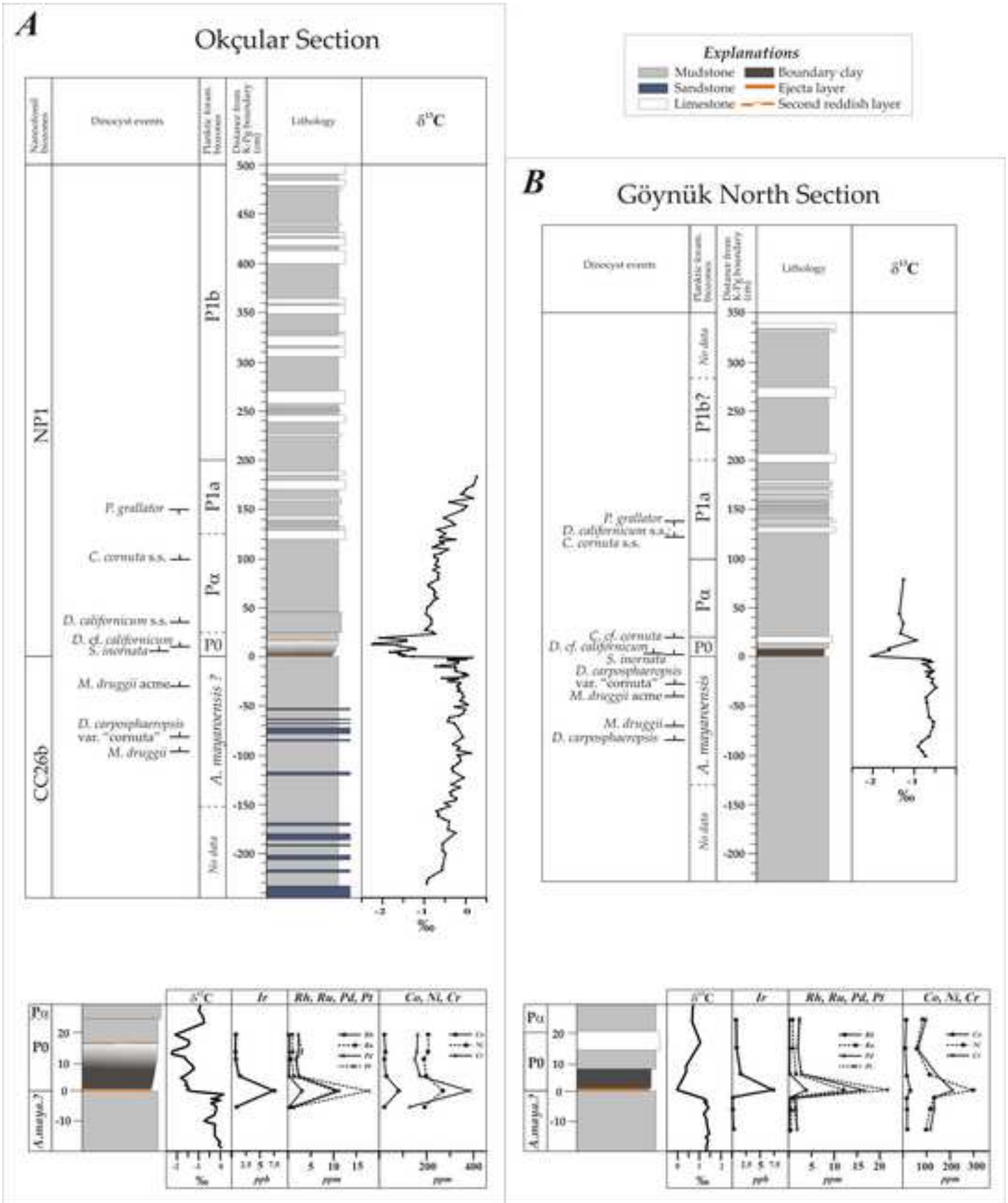

Figure5
Click here to download high resolution image

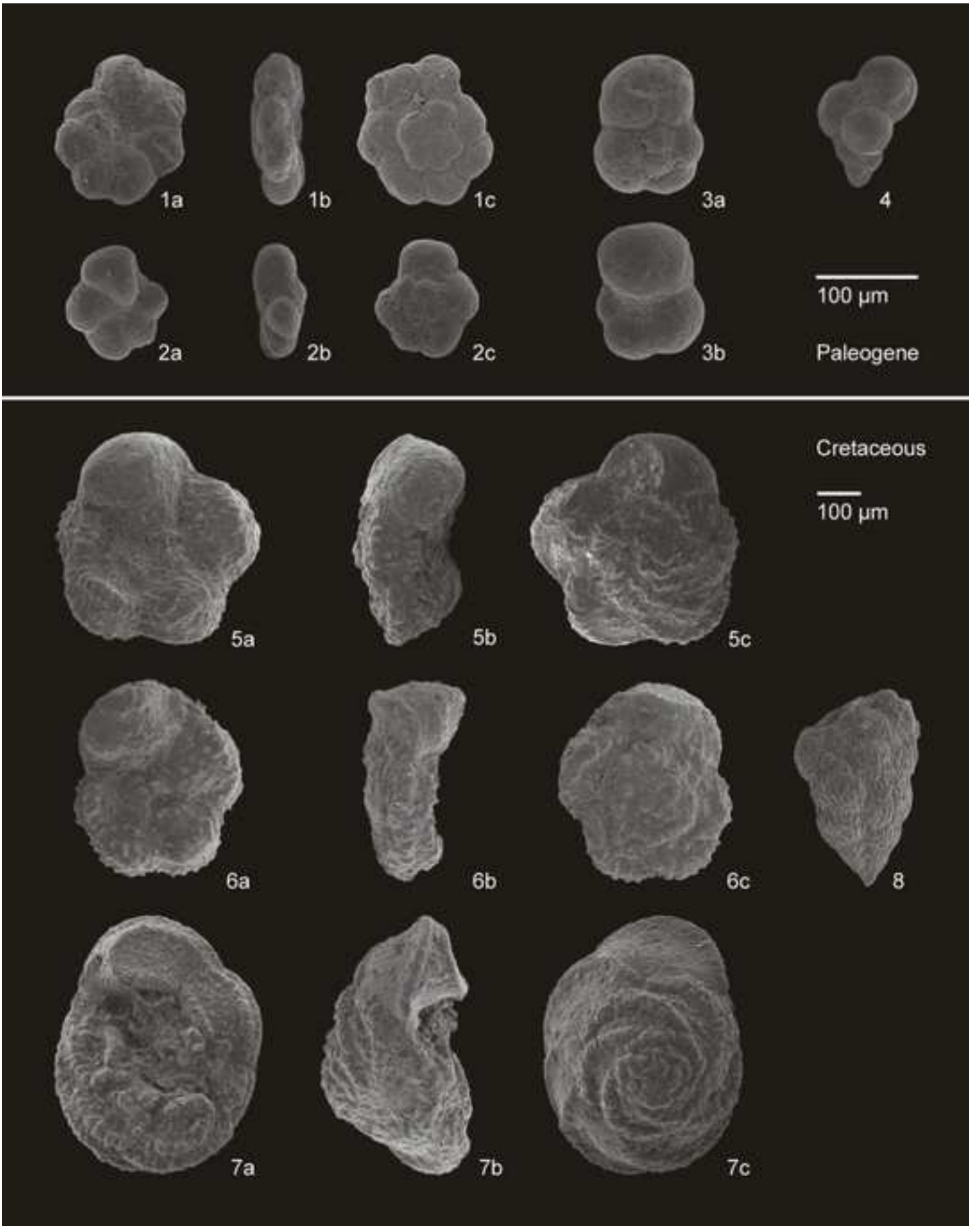

Figure6

Click here to download high resolution image

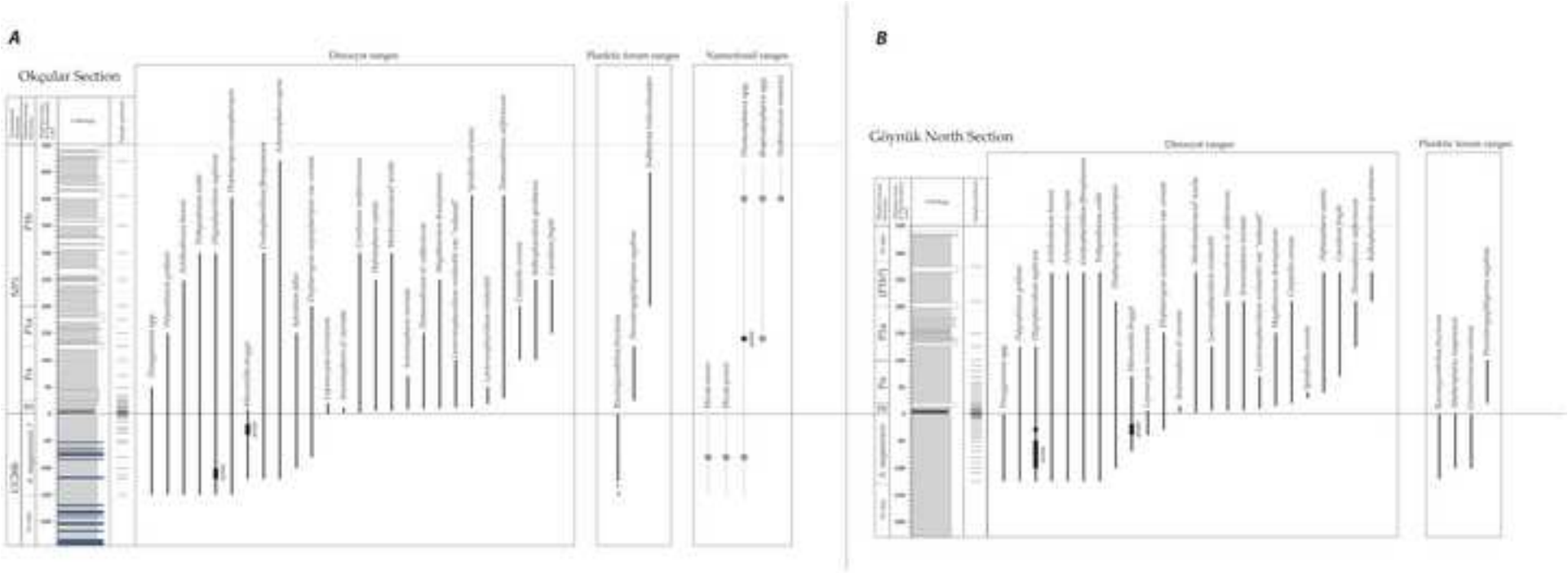

Figure7

Click here to download high resolution image

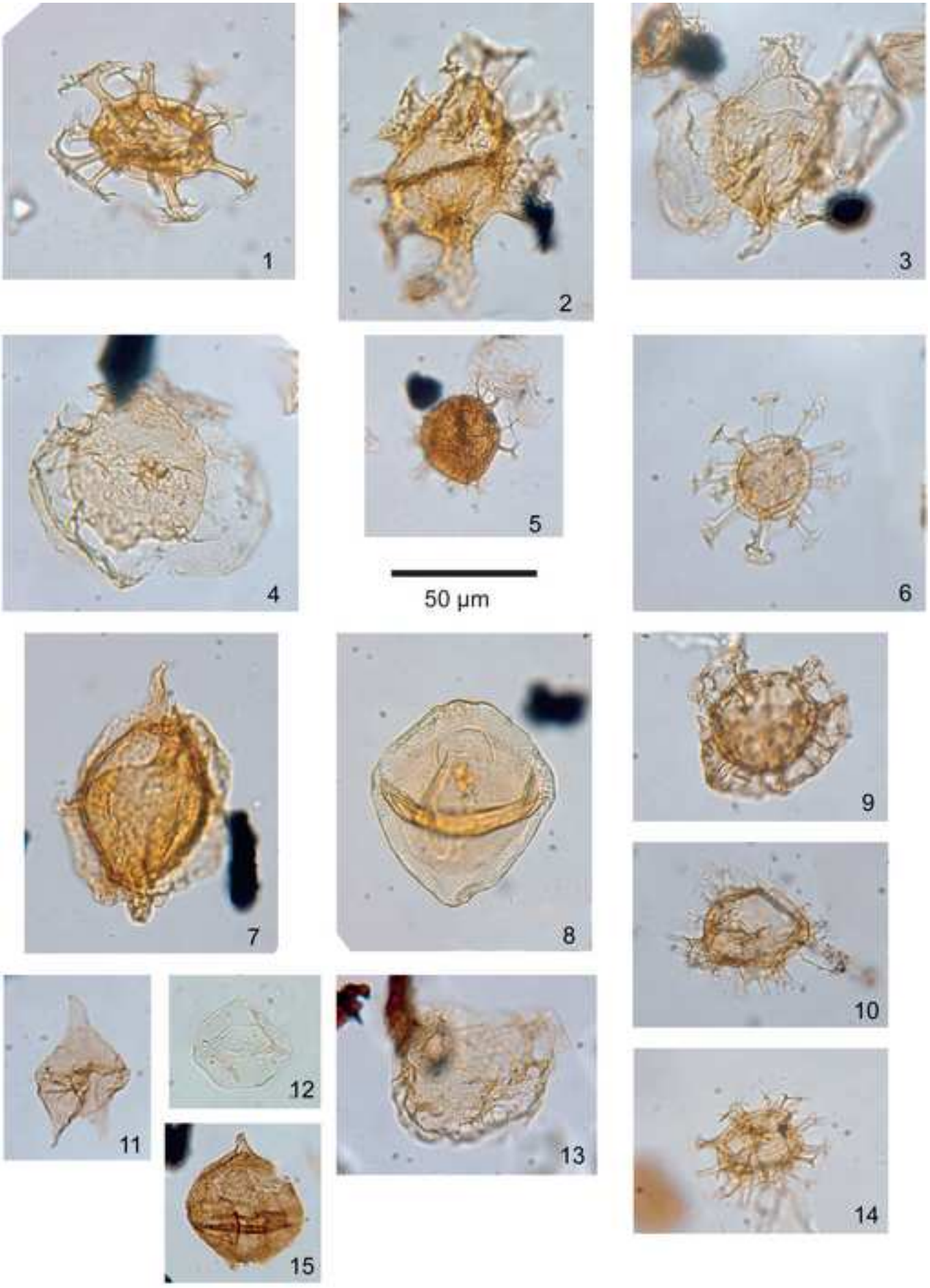

Figure8

Click here to download high resolution image

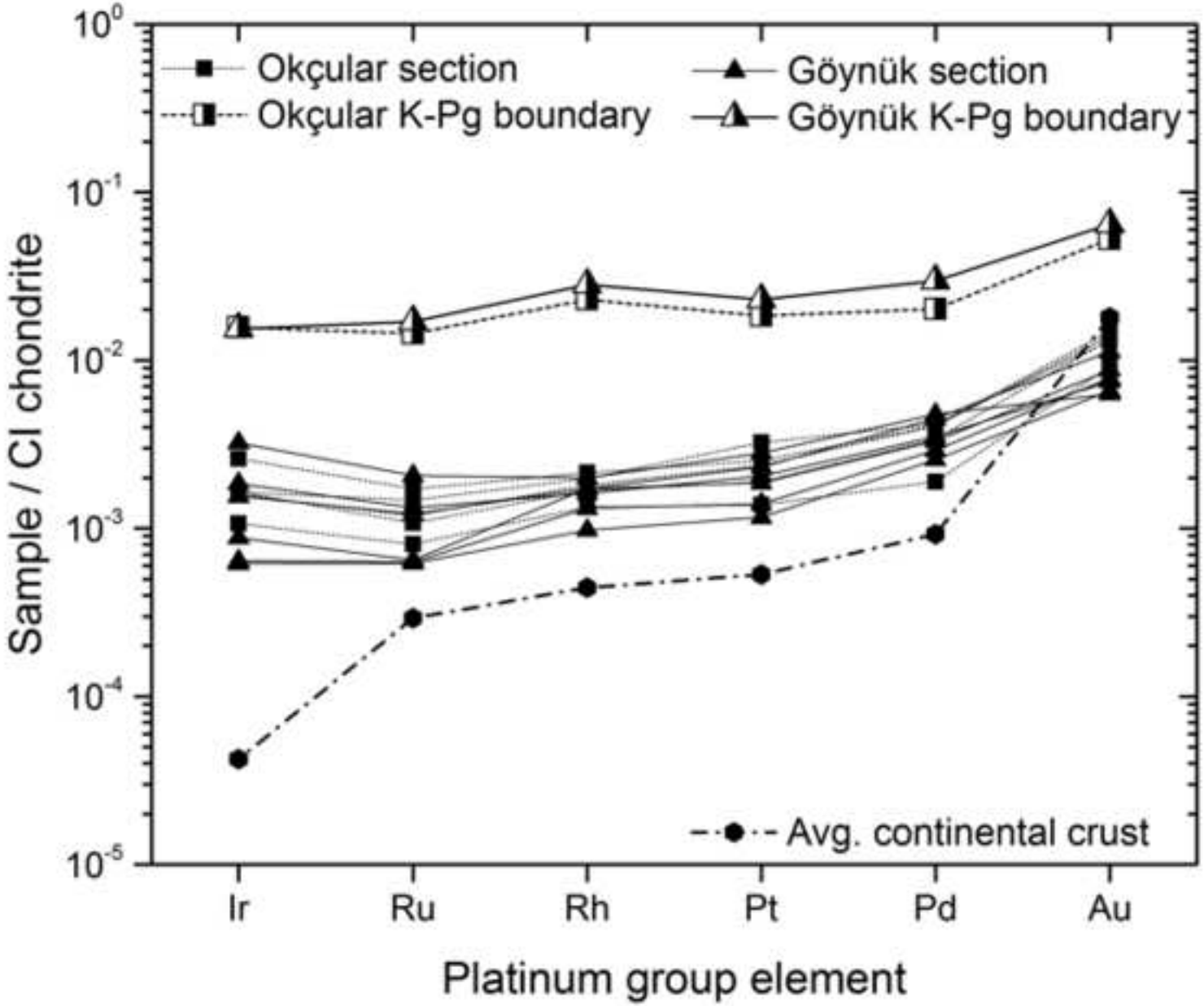

Figure9

Click here to download high resolution image

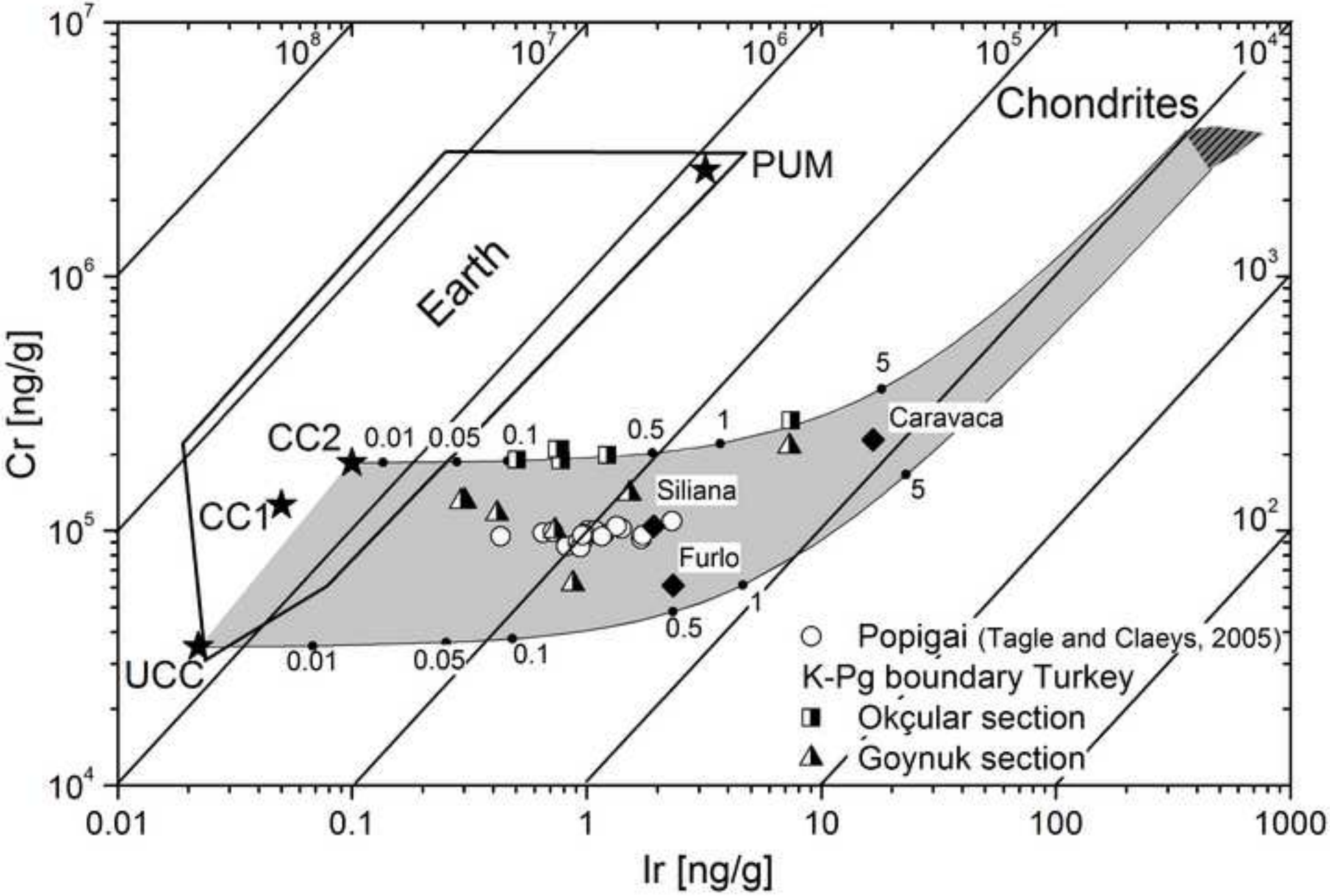

Figure10

Click here to download high resolution image

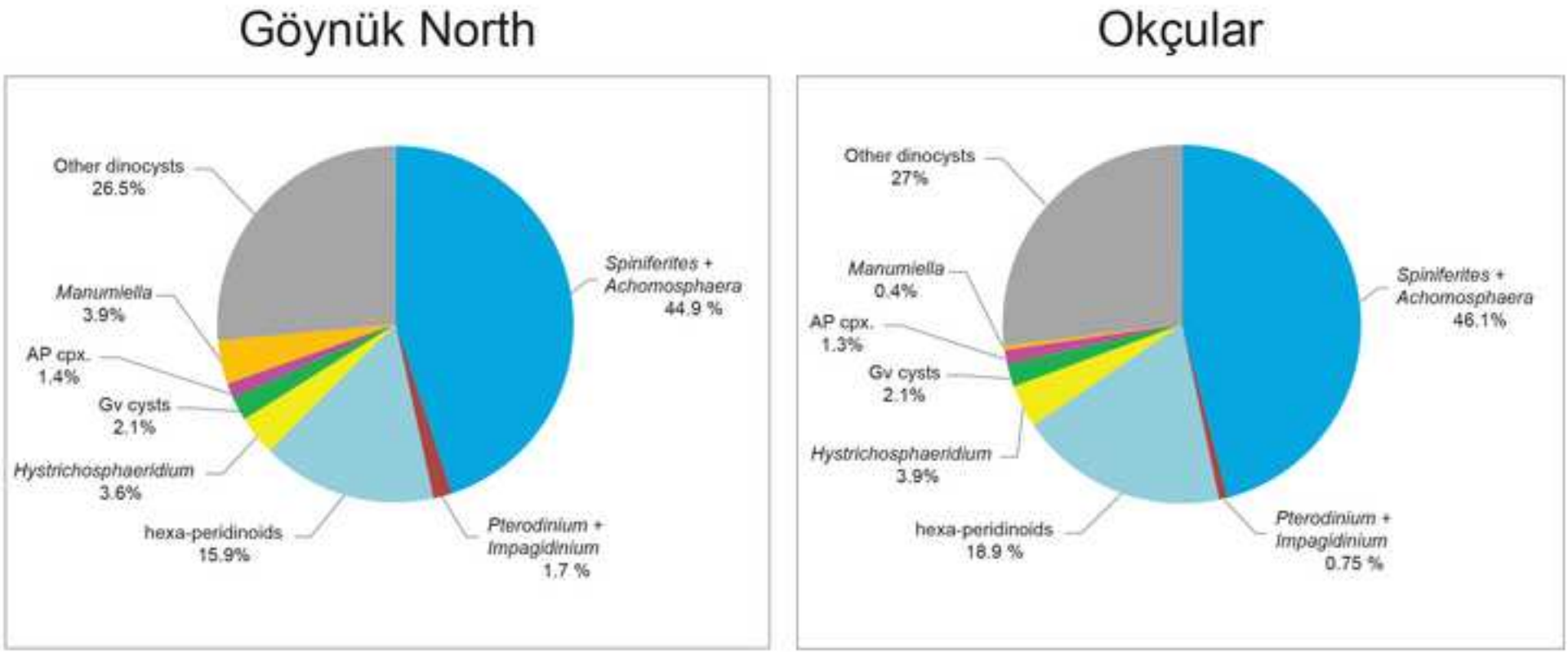

Figure11

Click here to download high resolution image

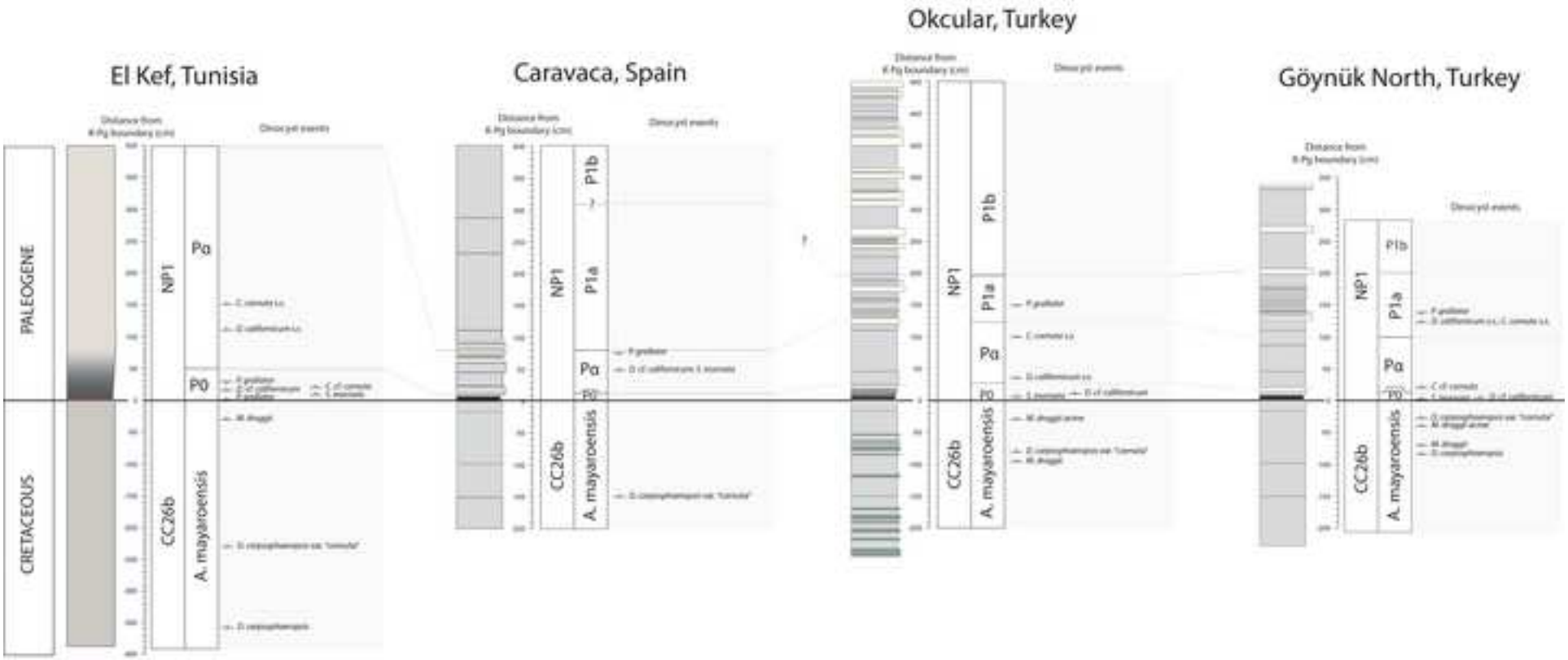

				Cretaceous forms																	survivors										incoming species													
Section	Code	Sample nr.	Depth (cm)	Watznaeria spp	Microrabdulus spp	Micula spp	M. murus	Micula prinsii	Nephrolites frequens	Retecapsa spp	Cribrosphaerella	Arkangeskiella	Prediscosphaera	Prediscosphaera stoveri	Eiffellithus turriseifelii	Eiffellithus eximius	Aspidulithus parcus	Lithraphidites quadratus	R. levii	Biscutum sp1	Cretaceous others	Thoracosphaera spp	Braarudosphaera spp.	Octolithus multiplus	Biantolithus sparsus	Biscutm spp	Cyclagelosphaera alta	Cyclagelosphaera reinarhardtii	Markalius apertus	Markalius inversus	Neochiastozygus spp	Neocrepidolithus spp	Zygodiscus spp	Neobiscutum parvulum/romeinii	Futyania petalosa	Cruciplacolithus primus <5um	Cruciplacolithus primus >5um	Cruciplacolithus intermedius	Cruciplacolithus edwardsii/asymetricus	Cruciplacolithus tenuis	Cruciplacolithus spp	Coccolithus pelagicus	Ericsonia subpertusa	Ericsonia cava (circolar)	Praeprinsius dimorphosus/tenuiculum	Chiasmolithus danicus	Cenozoic undetermined	**total**
Okcular section	OK-08	68	917.50	10	0	1	0	0	0	4	0	0	3	0	0	0	0	0	0	0	12	137	75	3	0	4	18	1	1	2	0	1	0	0	9	4	0	0	0	0	0	0	0	0	0	2	287
Okcular section	OK-08	59	629.50	18	0	6	0	0	0	2	0	0	3	0	0	0	0	0	0	0	6	93	152	3	0	2	2	0	2	3	1	0	0	0	7	3	0	0	0	0	0	0	0	0	0	2	305
Okcular section	OK-08	53	396.00	6	0	9	0	1	0	2	0	0	4	0	0	0	0	0	0	0	4	77	7	2	0	1	2	0	0	2	1	0	0	2	0	0	0	0	0	0	0	0	0	0	0	0	120
Okcular section	OK-08	46	138.00	0	0	0	0	0	0	0	0	0	0	0	0	0	0	0	0	0	8	111	1	0	0	0	2	1	0	2	0	1	0	0	0	0	0	0	0	0	0	0	0	0	0	0	126
Okcular section	OK-08	43D	-80.00	66	0	212	0	1	8	9	17	18	64	5	10	2	1	0	0	9	70	14	0	0	0	1	0	0	0	0	1	0	0	0	0	0	0	0	0	0	0	0	0	0	0	0	508
Okcular section	OK-08	43A	-270.00	57	0	130	0	1	0	4	1	4	40	4	0	1	0	0	0	5	46	11	0	0	0	0	0	0	0	0	0	0	0	0	0	0	0	0	0	0	0	0	0	0	0	0	304
Okcular section	OK-08	42C	-430.00	79	0	197	0	0	2	8	10	14	34	1	3	0	0	1	0	2	63	3	1	0	0	0	0	0	0	0	0	0	0	0	0	0	0	0	0	0	0	0	0	0	0	0	418

Appendix B. Systematic palynology - List of encountered dinocyst species and complexes

The generic allocation of taxa follows that cited in Fensome and Williams (2004) unless stated otherwise. Notes on certain taxa are provided.

Achilleodinium bianii Hultberg, 1985
Achomosphaera ramulifera (Deflandre, 1937) Evitt, 1973 **(Fig. 7.1)**
Achomosphaera sagena Davey and Williams, 1966
Achomosphaera spp. (pars)
Adnatosphaeridium buccinum Hultberg, 1985
Alisocysta circumtabulata (Drugg, 1967) Stover and Evitt, 1978
Alisocysta spp. (pars)
Alterbidinium acutulum (Wilson, 1967) Lentin and Williams, 1985
Andalusiella dubia (Jain & Millepied 1973) Lentin and Williams 1980
Andalusiella gabonensis (Stover & Evitt 1978) Wrenn and Hart 1988
Andalusiella mauthei Riegel, 1974
Andalusiella polymorpha (Malloy, 1972) Lentin and Williams, 1977
Apteodinium fallax (Morgenroth, 1968) Stover and Evitt, 1978
Areoligera coronata (Wetzel, 1933) Lejeune-Carpentier, 1938
Areoligera senonensis Lejeune-Carpentier, 1938
Areoligera spp. (pars)
Batiacasphaera rifensis Slimani 2008
Caligodinium amiculum Drugg, 1970
Cannosphaeropsis utinensis O. Wetzel, 1932
Carpatella cornuta Grigorovich, 1969
Carpatella cf. *cornuta*. This morphotype differs from *Carpatella cornuta* s.s. in having a less thick wall. In this study it is regarded as a transitional form between the taxa *Cribroperidinium* sp. A of Brinkhuis and Schiøler, 1996 and *Carpatella cornuta* s.s.
Carpatella septata Willumsen 2004
Cassidium fragile (Harris, 1965) Drugg, 1967
Cerodinium boloniense (Riegel, 1974) Lentin and Williams, 1989
Cerodinium diebelii subsp. *diebelii* (Alberti, 1959) Lentin and Williams, 1987
Cerodinium leptodermum (Vozzhennikova, 1963) Lentin and Williams, 1987
Cerodinium mediterraneum Slimani 2008
Cerodinium pannuceum (Stanley, 1965) Lentin and Williams, 1987
Cerodinium speciosum subsp. *speciosum* (Alberti, 1959) Lentin and Williams, 1987
Cerodinium striatum (Drugg, 1967) Lentin and Williams, 1987
Cerodinium spp. (pars)
Cladopyxidium saeptum (Morgenroth, 1968) Stover and Evitt, 1978
Cladopyxidium velatum Below, 1987
Cometodinium? *whitei* (Deflandre and Courteville, 1939) Stover and Evitt, 1978 - presumed reworked
Cordosphaeridium fibrospinosum Davey and Williams, 1966
Cordosphaeridium fibrospinosum var. *cornuta*. This taxon is distinguished from *Cordosphaeridium fibrospinosum* s.s. by the development of distinct apical and antapical horns. These typical forms appear to develop in the earliest Danian and have been described as" intermediate morphotype between *C. fibrospinosum* and *Damassadinium* spp of the *Cordosphaeridium fibrospinosum* Complex" by Brinkhuis and Sluijs 2009, plate 2 B
Cordosphaeridium inodes subsp. *inodes* (Klumpp, 1953) Eisenack, 1963
Coronifera striolata (Deflandre, 1937) Stover and Evitt, 1978
Cribroperidinium? *pyrum* (Drugg 1967) Stover and Evitt 1978
Cribroperidinium septatum (Hultberg 1985) Poulsen 1996
Cribroperidinium wetzelii (Lejeune-Carpentier, 1939) Helenes, 1984
Cribroperidinium wilsonii forma A of Slimani et al., 2011
Cribroperidinium sp. A of Brinkhuis & Schiøler 1996
Damassadinium californicum (Drugg 1967) Fensome et al. 1993

Damassadinium cf. *californicum*. This morphotype is distinguished from *Damassadinium californicum* s.s. by having a less broad process base. In this study it is regarded as a transitional form between the taxa *Cordosphaeridium fibrospinosum* var. *cornuta* and *Damassadinium californicum* s.s. These forms appear to evolve in the earliest Danian and can therefore be used as a marker species. **(Fig. 7.2)**

Deflandrea galeata (Lejeune-Carpentier 1942) Lentin and Williams 1973

Deflandrea tuberculata Hultberg, 1985

Diconodinium wilsonii (*Diconidinium parvum* in Wilson, 1974)

Dinogymnium acuminatum Evitt et al., 1967

Diphyes colligerum (Deflandre and Cookson 1955) Cookson 1965

Diphyes ?*recurvatum* May, 1980

Disphaerogena carposphaeropsis Wetzel 1933

Disphaerogena cf. *carposphaeropsis*. This taxon is distinguished from *Disphaerogena carposphaeropsis* s.s. in having a significantly more pronounced antapical horn. According to the emended diagnosis of Sarjeant, 1985, *Disphaerogena carposphaeropsis* s.s is characterized by an apical horn that is always longer than the antapical horn, by a ratio varying between 1.2:1 to 3:1. In the uppermost Maastrichtian samples, specimen occur with an antapical horn that is as long or longer than the apical horn. Since this form first appears in the uppermost Maastrichtian (i.e. Vellekoop et al., 2014), it is used as a stratigraphic marker in the present study. Since this form clearly belongs to the species *D. carposphaeropsis*, but is characterized by an antapical horn similar to the taxon *Carpatella cornuta*, we used the informal name '*Disphaerogena carposphaeropsis* variety "cornuta" in study. **(Fig. 7.3)**

Druggidium meerensis (Slimani and Louwye, 2011)

Exochospaeridium bifidum (Clarke and Verdier, 1967) Clarke et al., 1968

Exochosphaeridium phragmites Davey et al., 1966

Fibradinium annetorpense Morgenroth, 1968

Fibrocysta axialis (Eisenack 1965) Stover and Evitt 1978

Fibrocysta bipolaris (Cookson and Eisenack 1965) Stover and Evitt 1978

Fibrocysta licia (Jain et al. 1975) Stover and Evitt 1978

Fibrocysta spp. (pars)

Florentina ferox (Deflandre, 1937) Duxbury, 1980

Florentinia? *flosculus* (*Eurysphaeridium fibratum* in Wilson, 1974)

Florentinia mantellii (Davey and Williams, 1966)

Glaphyrocysta castelcasiensis (Corradini 1973) Michoux and Soncini in Fauconnier and Masure 2004

Glaphyrocysta perforata Hultberg and Malmgren 1985 **(Fig. 7.4)**

Glaphyrocysta retiintexta (Cookson, 1965) Stover and Evitt, 1978

Glaphyrocysta semitecta (Bujak in Bujak et al. 1980) Lentin and Williams 1981

Hafniasphaera septata (Cookson and Eisenack, 1967) Hansen, 1977 **(Fig. 7.5)**

Heterosphaeridium? heteracanthum (Deflandre and Cookson, 1955) Eisenack and Kjellström, 1971

Hystrichodinium pulchrum Deflandre, 1935. - presumed reworked

Hystrichokolpoma bulbosum (Ehrenberg, 1838)

Hystrichosphaeridium recurvatum (White 1842) Lejeune-Carpentier, 1940

Hystrichosphaeridium tubiferum (Ehrenberg, 1838) Deflandre, 1937 **(Fig. 7.6)**

Hystrichosphaeridium spp. (pars)

Hystrichosphaeropsis ovum Deflandre 1935

Hystrichostrogylon coninckii Heilmann-Clausen in Thomsen and Heilmann-Clausen, 1985

Impagidinium sp. 1 of Thomsen & Heilmann-Clausen 1985, following Slimani et al., 2010

Impagidinium spp. (pars)

Isabelidinium bakeri (Deflandre and Cookson, 1955) Lentin and Williams 1977

Kallosphaeridium yorubaense Jan du Chêne and Adediran, 1985

Lanternosphaeridium lanosum Morgenroth, 1966

Lanternosphaeridium reinhardtii Moshkovitz and Habib, 1993 **(Fig. 7.7)**

Lanternosphaeridium reinhardtii var. „reduced". This form of *Lanternosphaeridium reinhardtii* is characterized by a pericyst that is sheathed close to the endocyst. The description is of this

variety is already included in the original description of *Lanternosphaeridium reinhardtii* by Moshkovitz and Habib, 1993.

Lejeunecysta globosa Biffi and Grignani, 1983

Lejeunecysta hyalina (Gerlach 1961) Artzner and Dörhöfer, 1978

Lejeunecysta izerzenensis Slimani 2008

Lejeunecysta spp. (pars)

Manumiella conorata (Stover, 1974) Bujak and Davies, 1983

Manumiella druggii (Stover, 1974) Bujak and Davies, 1983, following Thorn et al., 2009 **(Fig. 7.8)**

Manumiella seelandica (Lange 1969) Bujak and Davies 1983, following Thorn et al., 2009

Membranilarnacia? *tenella* Morgenroth, 1968 **(Fig. 7.9)**

Membranilarnacia polycladiata (*Membranilarnacia multifibrata* in Wilson, 1974), following Slimani et al., 2011

Neonorthidium perforatum Marheinecke, 1992

Odontochitina operculata (O.Wetzel, 1933) Deflandre and Cookson, 1955 - presumed reworked

Oligosphaeridium complex (White, 1842) Davey and Williams, 1966

Oligosphaeridium saghirum Slimani et al., 2012. (?Homotryblium sp. of Brinkhuis and Zachariasse, 1988, p. 183, pl. 6, fig. 6, Oligosphaeridium sp. cf. Homotryblium sp. of Brinkhuis and Zachariasse 1988 of Slimani et al., 2010 p. 115, pl. 10, fig. 10).

Operculodinium centrocarpum (Deflandre & Cookson 1955) Wall 1967

Palaeocystodinium australinum (Cookson 1965) Lentin and Williams 1976

Palaeocystodinium golzowense Alberti 1961

Palaeocystodinium spp. (pars)

Palaeohystrichophora infusorioides Deflandre 1935 - presumed reworked

Palaeoperidinium pyrophorum (Ehrenberg, 1838) Sarjeant, 1967

Palaeotetradinium silicorum Deflandre, 1936

Palynodinium grallator Gocht, 1970 **(Fig. 7.10)**

Palynodinium cf. *grallator*. This morphotype differs from *Palynodinium grallator* s.s. in having less pronounced lateroventral protrusions

Pervosphaeridium spp.

Phelodinium magnificum (Stanley 1965) Stover and Evitt, 1978

Phelodinium pentagonale Corradini, 1973

Pierceites pentagonus (May 1980) Habib & Drugg 1987

Pterodinium cingulatum (O. Wetzel, 1933) Below, 1981

Pterodinum cretaceum Slimani, 2008

Pyxidinopsis spp.

Raetiaedinium truncigerum (Deflandre, 1937) Kirsch, 1991

Renidinium gracile Hultberg and Malmgren 1985

Riculacysta amplexa Kirsch, 1991

Senegalinium bicavatum Jain and Millepied 1973 **(Fig. 7.11)**

Senegalinium? *dilwynense* (Cookson and Eisenack 1965) Stover and Evitt 1978

Senegalinium laevigatum (Malloy 1972) Bujak and Davies 1983 **(Fig. 7.12)**

Senegalinium microgranulatum (Stanley 1965) Stover and Evitt 1978

Senegalinium obscurum (Drugg 1967) Stover and Evitt 1978

Senoniasphaera inornata (Drugg 1970) Stover and Evitt 1978 **(Fig. 7.13)**

Senoniasphaera cf. *inornata*. This morphotype differs from *Senoniasphaera inornata* s.s. in having a smaller size and thinner outer wall. In this study it is regarded as an early form of *Senoniasphaera inornata.*

Spinidinium densispinatum (Stanley 1965) following Sluijs et al., 2009

Spinidinium? pilatum (Stanley 1965) following Sluijs et al., 2009

Spiniferella cornuta (Gerlach, 1961)

Spiniferites pseudofurcatus (Klump, 1953) Sarjeant, 1970

Spiniferites ramosus (Ehrenberg 1838) Loeblich and Loeblich, 1966 **(Fig. 7.14)**

Spiniferites spp. (pars)

Spongidinium delitense (Ehrenberg, 1838) Deflandre, 1936

Surculosphaeridium? *longifurcatum* (Firtion, 1952) Davey et al., 1966

Tanyosphaeridium xanthiopyxides (Wetzel 1933) Stover and Evitt, 1978

Thalassiphora cf. *patula.* This taxon differs from *Thalassiphora patula* in having a periphragm that more or less surrounds the entire endophragm, instead of being closely oppressed at the dorsal site.

Thalassiphora cf. *pelagica.* This taxon differs from *Thalassiphora pelagica* in having a periphragm that more or less surrounds the entire endophragm, instead of being closely oppressed at the dorsal site. The typical "hole" in the ventral site of the periphragm is also missing.

Trabeculodinium quinquetrum Duxbury, 1980 following Mohammed et al., 2012.

Trichodinium castanea (Deflandre, 1935) Clarke and Verdier, 1967 - presumed reworked

Trithyrodinium evittii Drugg 1967 **(Fig. 7.15)**

Turnhosphaera hypoflata (Yun, 1981) following Slimani et al., 2011

Xiphophoridium alatum (Cookson and Eisenack, 1962) - presumed reworked

Appendix C.1. $\delta^{13}C$ data for Okçular and Göynük North sections

OKÇULAR SECTION										
Sample No	**Depth (cm)**	**$\delta^{13}C$ (‰)**		**Sample No**	**Depth (cm)**	**$\delta^{13}C$ (‰)**		**Sample No**	**Depth (cm)**	**$\delta^{13}C$ (‰)**
OK-1304	183,5	0,27		OK-1174	53,5	-0,83		OK-1094	-16,5	0,00
OK-1295	174,5	0,19		OK-1171	50,5	-0,93		OK-1093	-17,5	-0,07
OK-1292	171,5	0,03		OK-1164	43,5	-0,96		OK-1092	-18,5	0,05
OK-1288	167,5	-0,04		OK-1161	40,5	-0,86		OK-1090	-20,5	-0,07
OK-1286	165,5	-0,11		OK-1158	37,5	-0,82		OK-1089	-21,5	-0,57
OK-1282	161,5	0,17		OK-1154	33,5	-0,82		OK-1088	-22,5	-0,19
OK-1274	153,5	0,03		OK-1150	29,5	-0,92		OK-1086	-24,5	-0,42
OK-1270	149,5	-0,07		OK-1148	27,5	-0,97		OK-1084	-26,5	-0,13
OK-1262	141,5	-0,52		OK-1146	25,5	-0,80		OK-1081	-29,5	-0,20
OK-1258	137,5	-0,34		OK-1144	23,5	-0,73		OK-1080	-30,5	-0,19
OK-1255	134,5	-0,25		OK-1138	17,5	-1,45		OK-1078	-32,5	-0,15
OK-1250	129,5	-0,69		OK-1137	16,5	-1,42		OK-1077	-33,5	-0,16
OK-1246	125,5	-0,48		OK-1136	15,5	-1,55		OK-1076	-34,5	-0,19
OK-1242	121,5	-0,62		OK-1131	12	-1,64		OK-1074	-36,5	-0,08
OK-1240	119,5	-0,25		OK-1130	11	-1,56		OK-1070	-40,5	-0,06
OK-1238	117,5	-0,62		OK-1128	9	-1,26		OK-1066	-44,5	-0,14
OK-1236	115,5	-0,53		OK-1127	8	-1,20		OK-1065	-45,5	-0,06
OK-1234	113,5	-0,69		OK-1126	7	-1,39		OK-1062	-48,5	0,05
OK-1232	111,5	-0,79		OK-1125	6	-1,58		OK-1060	-50,5	-0,26
OK-1230	109,5	-0,42		OK-1124	5	-1,83		OK-1059	-53	-0,01
OK-1226	105,5	-0,59		OK-1123	4	-1,59		OK-1057	-57,5	-0,06
OK-1224	103,5	-0,76		OK-1122	3	-1,55		OK-1056	-59,5	-0,16
OK-1222	101,5	-0,74		OK-1121	2,5	-1,60		OK-1055	-61,5	-0,39
OK-1220	99,5	-0,67		OK-1120	2	-1,47		OK-1053	-65,5	-0,43
OK-1218	97,5	-0,68		OK-1118	1	-1,52		OK-1052	-67,5	-0,27
OK-1214	93,5	-0,73		OK-1117	0,5	-1,27		OK-1049	-72,5	-0,18
OK-1212	91,5	-0,65		OK-1114	-0,5	0,15		OK-1047	-81,5	-0,07
OK-1209	88,5	-0,78		OK-1113	-1	0,00		OK-1045	-88,5	-0,31
OK-1206	85,5	-0,65		OK-1112	-1,5	-0,11		OK-1044	-91,5	-0,15
OK-1202	81,5	-0,67		OK-1111	-2	-0,42		OK-1043	-94,5	-0,21
OK-1200	79,5	-0,65		OK-1110	-2,5	0,02		OK-1042	-97,5	0,12
OK-1196	75,5	-0,82		OK-1108	-3,5	-0,42		OK-1041	-99,5	-0,20
OK-1194	73,5	-0,90		OK-1107	-4	-0,28		OK-1040	-101,5	-0,15
OK-1192	71,5	-0,87		OK-1106	-4,5	-0,19		OK-1038	-105,5	-0,12
OK-1190	69,5	-0,79		OK-1105	-5,5	-0,17		OK-1037	-108,5	-0,19
OK-1188	67,5	-0,75		OK-1103	-7,5	-0,26		OK-1036	-111,5	-0,30
OK-1186	65,5	-0,73		OK-1102	-8,5	-0,57		OK-1035	-113,5	-0,33
OK-1184	63,5	-0,76		OK-1101	-9,5	-0,73		OK-1034	-116,5	-0,30
OK-1182	61,5	-0,74		OK-1100	-10,5	-0,24		OK-1032	-122,5	-0,05
OK-1180	59,5	-0,68		OK-1098	-12,5	-0,25		OK-1030	-129,5	-0,34
OK-1178	57,5	-0,78		OK-1096	-14,5	-0,24		OK-1029	-132,5	-0,14

OKÇULAR SECTION				GÖYNÜK NORTH SECTION		
Sample No	**Depth (cm)**	**$\delta^{13}C$ (‰)**		**Sample No**	**Depth (cm)**	**$\delta^{13}C$ (‰)**
OK-1028	-135,5	-0,31		GN-55	80	0,74
OK-1027	-137,5	-0,38		GN-48	45	0,63
OK-1026	-140,5	-0,35		GN-46	35	0,73
OK-1025	-143,5	-0,22		GN-44	25	0,66
OK-1024	-145,5	-0,25		GN-42	18	1,05
OK-1023	-148,5	-0,50		GN-39	10	0,38
OK-1022	-151,5	-0,38		GN-39A	10	0,47
OK-1021	-154,5	-0,57		GN-38	8	0,39
OK-1020	-156,5	-0,70		GN-35	2	-0,05
OK-1019	-159,5	-0,65		GN-33	-1	1,23
OK-1018	-161,5	-0,67		GN-32	-2	1,23
OK-1017	-164,5	-0,53		GN-32A	-2	1,36
OK-1016	-167	-0,40		GN-31	-4	1,43
OK-1014	-175,5	-0,42		GN-30A	-6	1,21
OK-1013	-178,5	-0,24		GN-29	-8	1,34
OK-1011	-189,5	-0,56		GN-27	-10	1,36
OK-1009	-196,5	-0,56		GN-26	-13	1,46
OK-1008	-199,5	-0,49		GN-25	-14	1,29
OK-1006	-212,5	-0,56		GN-24	-15	1,40
OK-1005	-216,5	-0,56		GN-23	-18	1,32
OK-1003	-224,5	-0,89		GN-22	-19	1,34
OK-1002	-227,5	-0,92		GN-21	-21	1,44
OK-1001	-230,5	-0,94		GN-20	-25	1,43
				GN-19	-30	1,53
				GN-17	-40	1,28
				GN-16	-45	1,30
				GN-13	-60	1,36
				GN-12	-65	1,46
				GN-11	-70	1,45
				GN-9	-80	1,35
				GN-8	-85	1,18
				GN-7	-90	1,09
				GN-6	-95	1,20
				GN-5	-100	1,27

Appendix C.2. Concentrations of Cr, Co, Ni, Ir, Ru, Pt, Rh, Pd and Au, for measured samples of the Okçular and Göynük North sections.

OKÇULAR									
Sample	**Depth (cm)**	**Ir**	**Ru**	**Pt**	**Rh**	**Pd**	**Cr**	**Ni**	**Co**
		(ppb)					**(ppm)**		
OK1140	19.5	0.751	0.853	2.274	0.245	2.291	209	164	22
OK1134*	13.5	0.774	1.058	3.108	0.267	2.349	210	161	27
OK1130	11	0.776	0.774	1.811	0.227	1.913	189	153	22
OK1124	5	1.228	1.233	2.429	0.289	2.303	199	174	27
OK1115	0	7.411	10.374	17.677	3.102	11.382	272	383	84
OK1105	-5.5	0.504	0.578	1.325	0.180	1.069	190	127	20
GÖYNÜK NORTH									
Sample	**Depth (cm)**	**Ir**	**Ru**	**Pt**	**Rh**	**Pd**	**Cr**	**Ni**	**Co**
		(ppb)					**(ppm)**		
GN +25	25	0.732	0.874	2.230	0.233	2.531	100	83	12
GN +15	15	0.873	0.950	1.969	0.218	1.972	62	56	9
GN +6	6	1.523	1.476	2.695	0.269	2.690	140	113	19
Goynuk KT	0.5	7.284	12.204	21.995	3.804	16.762	215	300	31
GN -2	-2	0.292	0.445	1.114	0.131	1.443	130	132	17
GN -6	-6	0.302	0.455	1.344	0.177	1.644	131	115	16
GN-13	-13	0.415	0.466	1.787	0.233	1.858	116	98	15

*** This sample represents the second reddish layer in the Okcular section.**